Journal of Medicinal Chemistry

Subscriber access provided by Stockholm University Library

Article

Novel pyrazolo[1,5-a]pyrimidines as translocator protein 18 kDa (TSPO) ligands: Synthesis, in vitro biological evaluation, [F]-labelling and in vivo neuroinflammation PET images.

Annelaure Damont, Vincent Medran-Navarrete, Fanny Cacheux, Bertrand Kuhnast, Géraldine Pottier, Nicholas Bernards, Frank Marguet, Frédéric Puech, Raphael Boisgard, and Frédéric Dollé

J. Med. Chem., **Just Accepted Manuscript** • DOI: 10.1021/acs.jmedchem.5b00932 • Publication Date (Web): 17 Aug 2015

Downloaded from http://pubs.acs.org on August 24, 2015

Just Accepted

"Just Accepted" manuscripts have been peer-reviewed and accepted for publication. They are posted online prior to technical editing, formatting for publication and author proofing. The American Chemical Society provides "Just Accepted" as a free service to the research community to expedite the dissemination of scientific material as soon as possible after acceptance. "Just Accepted" manuscripts appear in full in PDF format accompanied by an HTML abstract. "Just Accepted" manuscripts have been fully peer reviewed, but should not be considered the official version of record. They are accessible to all readers and citable by the Digital Object Identifier (DOI®). "Just Accepted" is an optional service offered to authors. Therefore, the "Just Accepted" Web site may not include all articles that will be published in the journal. After a manuscript is technically edited and formatted, it will be removed from the "Just Accepted" Web site and published as an ASAP article. Note that technical editing may introduce minor changes to the manuscript text and/or graphics which could affect content, and all legal disclaimers and ethical guidelines that apply to the journal pertain. ACS cannot be held responsible for errors or consequences arising from the use of information contained in these "Just Accepted" manuscripts.

ACS Publications

Journal of Medicinal Chemistry is published by the American Chemical Society. 1155 Sixteenth Street N.W., Washington, DC 20036

Published by American Chemical Society. Copyright © American Chemical Society. However, no copyright claim is made to original U.S. Government works, or works produced by employees of any Commonwealth realm Crown government in the course of their duties.

Novel pyrazolo[1,5-a]pyrimidines as translocator protein 18 kDa (TSPO) ligands: Synthesis, *in vitro* biological evaluation, [^{18}F]-labelling and *in vivo* neuroinflammation PET images.

Annelaure Damont,*[a,b] Vincent Medran-Navarrete,[a,b] Fanny Cacheux,[a,b] Bertrand Kuhnast,[a,b] Géraldine Pottier,[a,b] Nicholas Bernards,[a,b] Frank Marguet,[c] Frédéric Puech,[c] Raphaël Boisgard,[a,b] Frédéric Dollé.[a,b]

[a] *CEA, I2BM, Service Hospitalier Frédéric Joliot, Orsay, France.*

[b] *Inserm / CEA / Université Paris Sud, UMR 1023 – ERL 9218 CNRS, IMIV, Orsay, France.*

[c] *LGCR, Sanofi, Chilly-Mazarin, France.*

■ ABSTRACT

A series of novel pyrazolo[1,5-a]pyrimidines, closely related to *N*,*N*-diethyl-2-(2-(4-(2-fluoroethoxy)phenyl)-5,7-dimethylpyrazolo[1,5-a]pyrimidin-3-yl)acetamide (**2**, DPA-714), were synthesised and biologically *in vitro* evaluated for their potential to bind the translocator protein 18 kDa (TSPO), a protein today recognized as an early biomarker of neuroinflammatory processes. This series is composed of fluoroalkyl- and fluoroalkynyl- analogues, prepared from a common iodinated intermediate *via* Sonogashira coupling reactions. All derivatives displayed subnanomolar affinity for the TSPO (0.37 to 0.86 nM), comparable to that of **2** (0.91 nM). Two of them were radiolabelled with fluorine-18 and their biodistribution was investigated by *in vitro* autoradiography and positron emission tomography (PET) imaging on a rodent model of neuroinflammation. Brain uptake and

local accumulation of both compounds in the AMPA-mediated lesion confirm their potential as *in vivo* PET-radiotracers. In particular, [^{18}F]**23** exhibited a significantly higher ipsi- to contralateral ratio at 60 minutes than the parent molecule [^{18}F]**2** *in vivo*.

■ INTRODUCTION

Nearly all brain diseases reveal pronounced changes in the functional states of glial cells and most prominent is the presence of activated microglia in areas of progressive disease or tissue destruction. Microglia activation is characterized by the overexpression of the translocator protein 18 kDa (TSPO) on the outer mitochondrial membranes, supporting for over two decades considerable efforts in the design of radioligands for the *in vivo* imaging of this pharmacological target by Positron Emission Tomography (PET).[1]

Today, the isoquinoline carboxamide [^{11}C]**1** ([^{11}C]PK11195[1]) is still the most widely used PET-radioligand to localise TSPO and visualise its expression level changes *in vivo*. Nevertheless the non-optimal profile of this radioligand, especially with regard to the high level of non-specific binding resulting in a poor signal to noise ratio obtained *in vivo* during PET studies, encourage the search for more adequate radioligands. Few analogues of **1** labelled with a short-lived isotope have been described so far, among which [^{11}C]PK11211[2], [^{11}C]PK14105[2] and [^{18}F]PK14105[2] or more recently [^{11}C]PK13015[3], [^{11}C]PK12090[3] and [^{11}C]PK14045[3] (Figure 1). SAR studies are still on-going to identify new lead TSPO ligands derived from **1** such as 4-phenylquinazoline-2-carboxamides[4,5] or derivatives featuring a 2-arylquinoline scaffold.[6] Besides these analogues of **1**, a number of new compounds, belonging to various chemical families, have also been prepared and investigated as TSPO ligands. Among them, some have been labelled (usually on the basis of their promising *in vitro* profiles) either with carbon-11 ($T_{1/2}$ = 20.4 min.) or with the longer half-life isotope fluorine-18 ($T_{1/2}$

= 109.8 min.), and *in vivo* evaluated. The early discovery of the benzodiazepine Ro5-4864,[7,8] a chlorinated analogue of diazepam, as high affinity TSPO ligand and its carbon-11-labelling in 1984,[9] have encouraged the development of a series of compounds of which structures result from the cleavage of the diazepine ring, giving rise to the phenoxyarylacetamides family. [^{11}C]DAA1106[10–12] was the first carbon-11-labelled representative of this series to emerge because of its subnanomolar binding affinity and selectivity for the TSPO. Its initial development was concomitant with the synthesis of two fluorine-18-analogues, [^{18}F]FMDAA1106[13] and [^{18}F]FEDAA1106,[13] which was rapidly followed by the preparation of [^{18}F]PBR06[14,15] in 2005 and [^{18}F]DAA1106[16] in 2007. So far, other closely related compounds have appeared in the literature for their high potential to *in vivo* PET-image the TSPO. For examples, [^{11}C]PBR28,[17,18] a carbon-11-labelled phenoxypyridinyl acetamide, was proposed by Briard *et al.*, followed by two radiofluorinated analogues: [^{18}F]FEPPA[19], and more recently 6-[^{18}F]F-PBR28.[20]

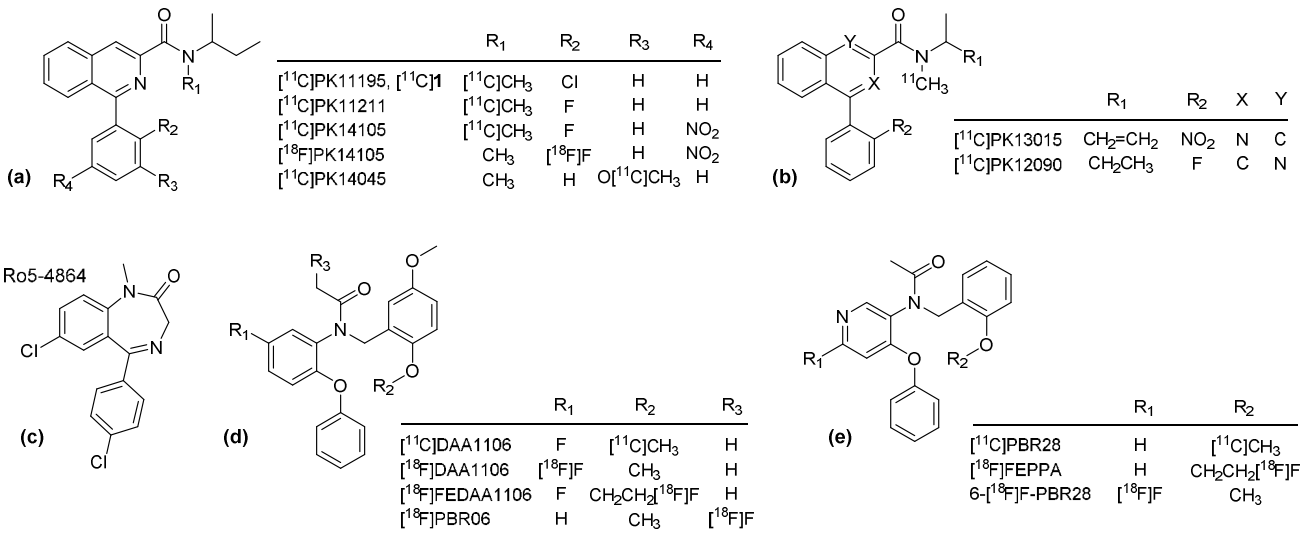

Figure 1. Representative examples of TSPO ligands belonging to the following families: (a) isoquinolines, including [^{11}C]**1**, (b) other analogues of **1**, (c) a benzodiazepine, (d) phenoxyphenylacetamides and (e) phenoxypyridinylacetamides.

Besides these derivatives inspired from **1** or benzodiazepines, TSPO PET imaging has encouraged the design of many other radioligands that share a number of common structural characteristics and can be grouped together around the schematic architectural representation proposed in Figure 2 (a). Indeed, they exhibit a multicyclic heteroaromatic planar skeleton as central molecular core and have the particularity to commonly feature an acetamide function, linked to the heteroaromatic backbone, whose presence seems to be a requirement for efficient binding with the protein.[21] It is also interesting to note that most of these molecules display an aromatic ring directly attached to their planar scaffold. The first radiolabelled molecules of this kind were inspired from the structure of the imidazopyridine alpidem that binds both peripheral (TSPO) and central (CBR) benzodiazepine receptors. Within this series, [^{11}C]CLINME[22], [^{11}C]PBR170[23–26] and [^{11}C]-A[27] are carbon-11-labelled representative examples while [^{18}F]PBR111[28,29] and [^{18}F]PBR102[28,29] are fluorine-18-labelled specimens. Beside imidazopyridine acetamides, a number of bioisosteric structures have also been explored as potential scaffolds allowing specific and efficient binding to the TSPO, such as pyrazolopyrimidine or imidazopyridazine acetamides. The carbon-11-labelled compound [^{11}C]DPA-713[30-35] and the fluorine-18 close analogues [^{18}F]**2** ([^{18}F]DPA-714)[36-39] and [^{18}F]VUIIS1008[40,41] are illustrations of TSPO imaging agents belonging to the pyrazolopyrimidine acetamides family, whereas [^{18}F]PBR132[42] is an example of imidazopyridazine acetamide radioligand. A number of 2-aryl-indole-3-acetamide derivatives, also known as FGIN-1 class compounds[43], were screened against TSPO and were shown to display high affinity and selectivity. Recently, conformationally constrained versions of this series of molecules have been explored as novel TSPO ligands and one of them has been labelled at its methylindole moiety (Figure 2).[44] In this series, compounds feature a glyoxylamide moiety in replacement of the acetamide motif rendering the structures less flexible in hopes of increased affinity and selectivity toward the TSPO. Other closely related structures,

resulting from the fusion of the indole moiety with a pyridazine ring, have been proposed as potential probes to image TSPO expression. [^{11}C]SSR180575[45] is a carbon-11-labelled illustration of this phenyl-pyridazinoindole acetamide family. Another indoleacetamide, [^{18}F]GE-180[46], bearing a labelling at the *N*-indole position has recently been reported. Unlike the other previously mentioned radioligands, it does not share the particularity of featuring a freely rotating aryl group linked to the main heteroaromatic core of the molecule and was conformationally constrained by cyclisation via an α-branching of the acetamide part. Finally, a number of 2-aryl-8-oxodihydropurine acetamides have also been radiolabelled and evaluated for their potential to selectively image the TSPO expression. [^{11}C]AC-5216,[47] [^{18}F]FEDAC[48] and [^{18}F]FAC[48] are representative examples belonging to the latter series.

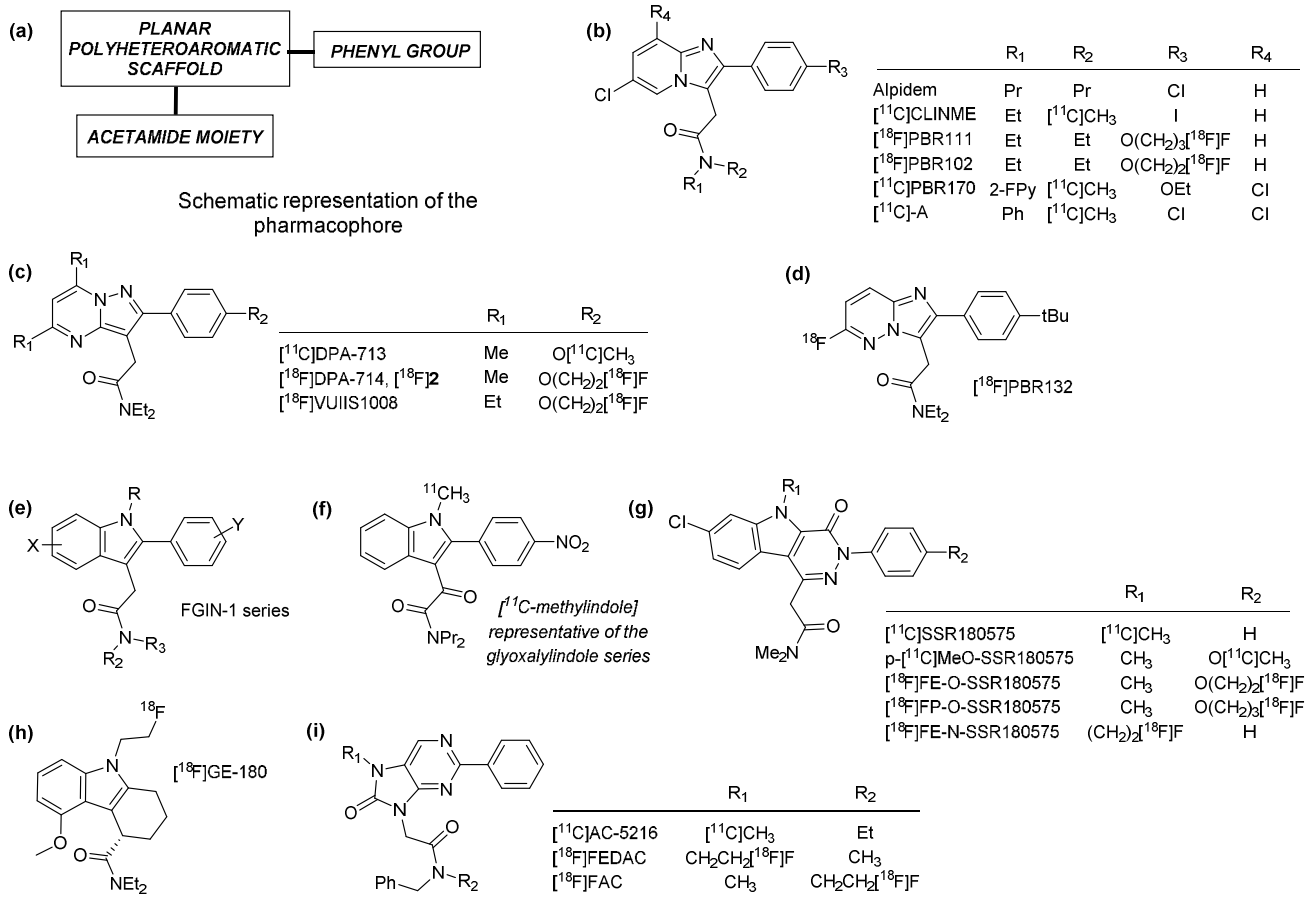

	R_1	R_2	R_3	R_4
Alpidem	Pr	Pr	Cl	H
[^{11}C]CLINME	Et	[^{11}C]CH_3	I	H
[^{18}F]PBR111	Et	Et	$O(CH_2)_3$[^{18}F]F	H
[^{18}F]PBR102	Et	Et	$O(CH_2)_2$[^{18}F]F	H
[^{11}C]PBR170	2-FPy	[^{11}C]CH_3	OEt	Cl
[^{11}C]-A	Ph	[^{11}C]CH_3	Cl	Cl

	R_1	R_2
[^{11}C]DPA-713	Me	O[^{11}C]CH_3
[^{18}F]DPA-714, [^{18}F]**2**	Me	$O(CH_2)_2$[^{18}F]F
[^{18}F]VUIIS1008	Et	$O(CH_2)_2$[^{18}F]F

	R_1	R_2
[^{11}C]SSR180575	[^{11}C]CH_3	H
p-[^{11}C]MeO-SSR180575	CH_3	O[^{11}C]CH_3
[^{18}F]FE-O-SSR180575	CH_3	$O(CH_2)_2$[^{18}F]F
[^{18}F]FP-O-SSR180575	CH_3	$O(CH_2)_3$[^{18}F]F
[^{18}F]FE-N-SSR180575	$(CH_2)_2$[^{18}F]F	H

	R_1	R_2
[^{11}C]AC-5216	[^{11}C]CH_3	Et
[^{18}F]FEDAC	CH_2CH_2[^{18}F]F	CH_3
[^{18}F]FAC	CH_3	CH_2CH_2[^{18}F]F

Figure 2. (a) Schematic representation of a number of TSPO ligands and some representative examples belonging to the following families: (b) 2-aryl-imidazo[1,2-a]pyridine-3-acetamides, (c) 2-aryl-pyrazolo[1,5-a]pyrimidine-3-acetamides, (d) 2-aryl-imidazo[1,2-b]pyridazine-3-acetamides, (e) 2-aryl-indole-3-acetamides, (f) 2-aryl-indole-3-glyoxylamides, (g) 3-aryl-pyridazino[4,5-b]indole-5-acetamides, (h) α-branched-indole acetamides and (i) 2-(8-oxo-2-aryl-dihydropurine) acetamides.

Among all these series of compounds, we have been particularly interested in the design of novel 3,5-dimethylpyrazolo[1,5-*a*]pyrimidin-3-ylacetamide (DPA) specimens, leading to the discovery of the fluoroethoxy derivative [^{18}F]**2**,[38–39] today considered as a serious challenger of [^{11}C]**1**. However, recent studies clearly demonstrate that this compound is rapidly and extensively *in vivo* metabolised in both rodents (rats) and non-human primates (baboons).[49] The major radiometabolites generated have been identified: they mainly result from oxidation at the sensitive methyl groups of the DPA scaffold or oxidation at the alpha-position of the nitrogen atom of the acetamide moiety leading to *N*-deethylated metabolites. These metabolites have been proved not to cross the human BBB. Nevertheless and in a lesser extent, the brain-penetrant radiometabolite [^{18}F]fluoroacetate has also been shown to be liberated.[49] Indeed, [^{18}F]**2** is also subjected to oxidation at the alpha-position of the oxygen bridging the fluorine-18 atom to the DPA scaffold (ether linkage). The presence of [^{18}F]fluoroacetate as well as its further *in vivo* conversion to [^{18}F]fluoride may reduce the PET image quality. Thus, within the present work, novel DPA analogues were designed by replacing the ether linkage of **2** with fragments preventing metabolic fluoroacetate release. Two sub-series of compounds were prepared: four fluoroalkyl- and four fluoroalkynyl- derivatives of **2**. Their TSPO binding and selectivity versus the CBR were evaluated *in vitro* as well as their lipophilicity. *In vitro* metabolism studies were also performed, using human, rat and mouse microsomes. Based on the *in*

vitro data obtained, two representatives, one in each sub-class of analogues, were selected for radiolabelling with fluorine-18 to evaluate their potency as TSPO radiotracers in animal models.

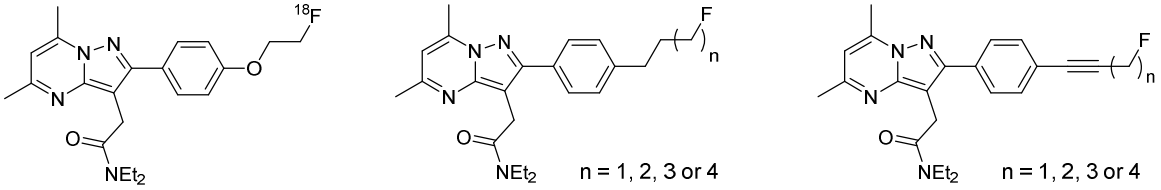

[^{18}F]**2** *Fluoroalkyl- analogues* *Fluoroalkynyl- analogues*

Figure 3. Structures of [^{18}F]**2** and the investigated new fluoroalkyl- and fluoroakynyl- analogues.

■ RESULTS AND DISCUSSION

Chemistry. Compound **12**, the structurally closest analogue of **2** in the fluoroalkyl series, featuring a methylene group in replacement of the oxygen atom, was the first candidate of the new series to be prepared. The initial synthetic route employed for its preparation is depicted on scheme 1. From commercially available methyl 4-hydroxybenzoate, the iodopropoxy or bromopropoxy derivatives **3** and **4** were obtained in good yields (72 and 83 % respectively) by *O*-alkylation with the appropriate 1,3-dihalopropane in presence of a base in acetone. They were subsequently converted to methyl 4-(3-hydroxypropyl)benzoate (**5**) *via* aryl translocation from oxygen to carbon using standard radical generating conditions (13-18 %).[50] The resulting alcohol **5** was subsequently protected with *tert*-butyldiphenylsilyl chloride (TBDPSCl) to give compound **6** (80 % yield). Reaction of **6** with sodium methoxide in refluxing acetonitrile yielded nitrile **7** which was alkylated with *N*,*N*-diethylchloroacetamide to afford amide **8** in sufficient amount (28 % over 2 steps). A first condensation reaction was conducted between **8** and hydrazine hydrochloride to afford the aminopyrazole **9** in excellent yield (95 %). The latter compound was subsequently submitted to a second condensation step using pentan-2,4-dione to achieve the construction of the DPA scaffold and generate the pyrazolo[1,5-a]pyrimidine **10** (75 % yield) to which hydroxyl group was subsequently

unprotected with tetrabutylammonium fluoride in THF to afford **11** (66 % yield). Finally, alcohol **11** was treated with the deoxofluorinating agent bis(2-methoxyethyl)aminosulfur trifluoride in toluene at room temperature to afford compound **12** in 52 % yield.

Scheme 1. First synthetic pathway explored for the preparation of compound 12[a].

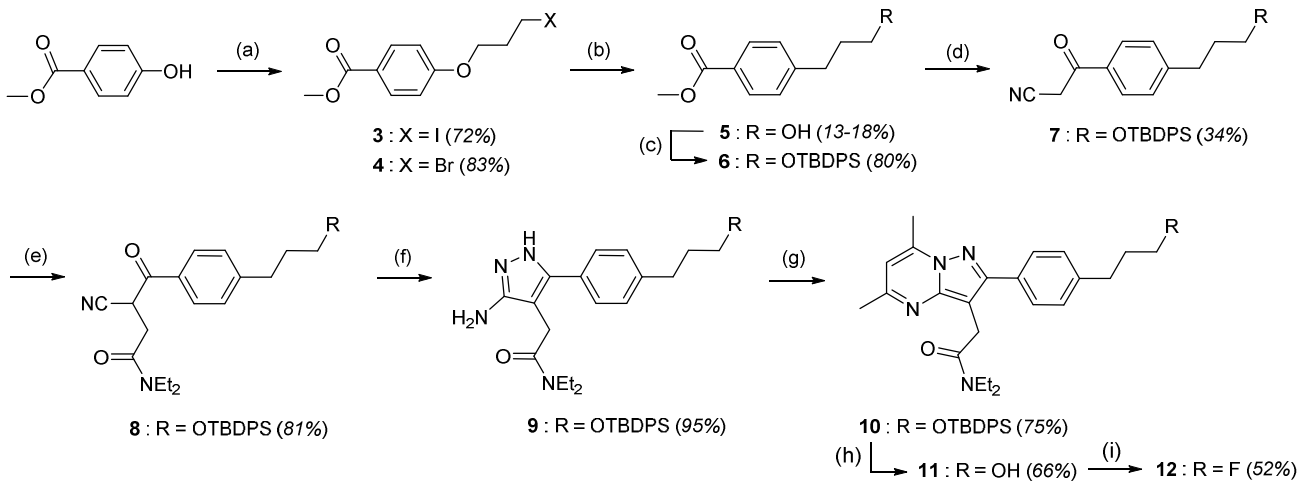

[a]Reaction conditions: (a) 1,3-diiodopropane or 1,3-dibromopropane, K_2CO_3, acetone, 50 °C, 16 h; (b) Bu_3SnH, AIBN, toluene, reflux, 12 h; (c) TBDPSCl, pyridine, r.t., 4 h; (d) NaOMe, CH_3CN, reflux, 4 h; (e) *N*,*N*-diethyl-chloroacetamide, NaOH, EtOH, H_2O, 75 °C, 12 h; (f) $NH_2NH_2.H_2O$, AcOH, EtOH, 60 °C, 3 h; (g) pentan-2,4-dione, EtOH, 60 °C, 16 h; (h) TBAF, THF, r.t., 8 h; (i) bis(2-methoxyethyl)aminosulfur trifluoride, toluene, r.t., 6 h.

Afterwards, a more general synthetic method was developed for the preparation of the fluoroalkyl- and fluoroalkynyl- analogues of **2**, *via* a common iodophenyl intermediate (compound **16**), as depicted in scheme 2. This alternative pathway was also reused for the preparation of **12** at a higher scale stimulated by the need to increase its global yield of production due to the very low yield of the translocation reaction (13 to 18 %). Thus, obtainment of cyanoketone **13** was achieved *via* formation of the lithium salt of acetonitrile by treatment with *n*-BuLi in THF at -60 °C followed by reaction

with commercial methyl 4-iodobenzoate at -45 °C (70 % yield). Subsequent alkylation of **13** with *N*,*N*-diethylchloroacetamide in presence of sodium hydroxide and sodium iodide in ethanol yielded amide **14** (54 % yield) which, upon reaction with hydrazine monohydrate in refluxing ethanol with a catalytic amount of acetic acid, afforded aminopyrazole **15** in 77 % yield. Pyrazolo[1,5-a]pyrimidine **16** was efficiently obtained (78 % yield) by reacting **15** with pentan-2,4-dione in refluxing ethanol. Sonogashira coupling of **16** with the appropriate alkynol using $Pd(PPh_3)_2Cl_2$ and CuI in triethylamine afforded the expected hydroxyalkynylphenyl compounds **17**, **18**, **19** and **20** in good yields (64 %, 78 %, 69 % and 80 % respectively). Alcohols **17**, **18**, **19** and **20** were then reacted with bis(2-methoxyethyl)aminosulfur trifluoride in dichloromethane to generate the corresponding fluorine derivatives **21**, **22**, **23** and **24** (8 to 62 % yields). They were also hydrogenated in methanol in presence of Pd/C for reduction of the triple bond to lead to their hydroxyalkylphenyl counterparts **11**, **25**, **26** and **27** respectively (40 to 92% yields). It is worth noting that compound **21** was not easily accessible using this strategy since reaction of bis(2-methoxyethyl)aminosulfur trifluoride with the propargylic alcohol **17** led to side products difficult to separate from the expected fluoropropynyl analogue **21**. Finally, in the alkyl- series, alcohols **11**, **25**, **26** and **27** were converted to their fluorinated counterparts by deoxofluorination in dichloromethane to give fluoropropyl-compound **12**, fluorobutyl-compound **28**, fluoropentyl-compound **29** and fluorohexyl-compound **30** in moderate yields (43 to 58 %).

Scheme 2. Synthetic preparation of fluoroalkynyl- (21-24) and fluoroalkyl- (12, 28-30) analogues[a].

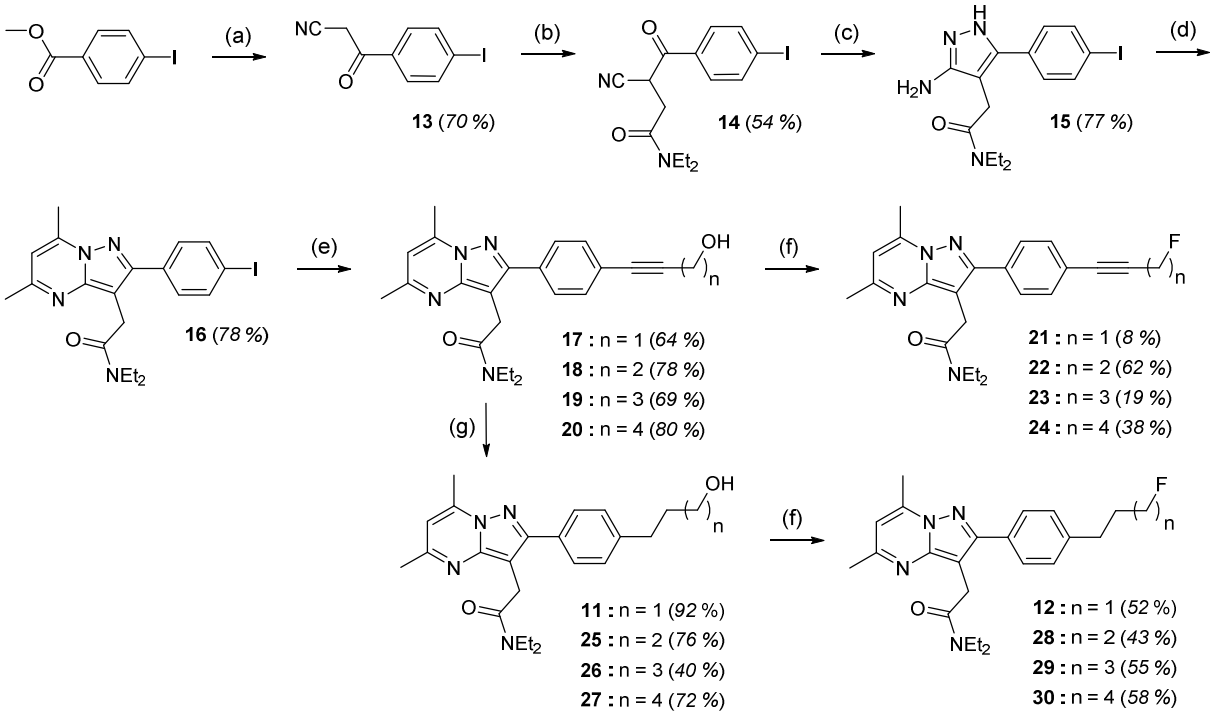

[a]Reaction conditions: (a) *n*-BuLi, CH_3CN, THF, -65 °C, 30 min then methyl 4-iodobenzoate, -65 °C to -45 °C, 2 h; (b) NaOH, EtOH, r.t., 15 min then *N*,*N*-diethyl-chloroacetamide, NaI, r.t., 4 d.; (c) $N_2H_4.H_2O$, AcOH, EtOH, 80 °C, 5-8 h; (d) acetylacetone, EtOH, 80 °C, 5 h; (e) alkynyl alcohol, CuI, $Pd(PPh_3)_2Cl_2$, Et_2NH, r.t., 24 h; (f) bis(2-methoxyethyl)aminosulfur trifluoride, CH_2Cl_2, r.t., 2-4 d.; (g) H_2, Pd/C 10 %, CH_2Cl_2, r.t., 48 h.

***In vitro* binding assays.** The binding affinity for the TSPO of these novel analogues of **2** were measured by competition experiments against [^{3}H]**1** in membrane homogenates of rat heart. The binding affinity of the newly synthesised compounds were also evaluated for the CBR by competitive binding assays against [^{3}H]flunitrazepam using membrane homogenates of rat cerebral cortex. The inhibition constants (Ki_{TSPO}) and percentage of inhibition at 1 μM (CBR) were determined for each ligand and are reported in Table 1. The lipophilicity parameter $LogD_{7.4}$ was also evaluated for this

new series of compounds on the basis of their HPLC retention times and the corresponding lipophilic efficiencies (LipE) were calculated.[51] Data are summarized in Table 1.

Table 1. *In vitro* competitive binding assays, lipophilicity determination and LipE calculation.

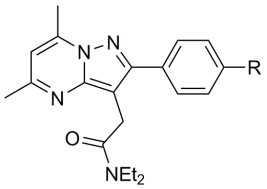

Series	Ligand	R	TSPO K_i (*nM*)[a,b]	CBR *% inhib. at 1μM*[c]	$LogD_{7.4}$[d]	TSPO pIC_{50}	LipE[e]
	2	O-$(CH_2)_2$-F	0.91 ± 0.08	0 %	2.89	9.00	6.11
Alkyl-	**12**	$(CH_2)_3$-F	0.37 ± 0.02	0 %	3.51	9.39	5.88
	28	$(CH_2)_4$-F	0.86 ± 0.06	0 %	3.90	9.02	5.12
	29	$(CH_2)_5$-F	0.54 ± 0.03	3 %	4.31	9.22	4.91
	30	$(CH_2)_6$-F	0.45 ± 0.03	12 %	4.70	9.30	4.60
Alkynyl-	**21**	C≡C-CH_2-F	0.54 ± 0.04	0 %	3.61	9.22	5.61
	22	C≡C-$(CH_2)_2$-F	0.74 ± 0.06	0 %	3.67	9.09	5.42
	23	C≡C-$(CH_2)_3$-F	0.35 ± 0.04	0 %	4.06	9.41	5.35
	24	C≡C-$(CH_2)_4$-F	0.79 ± 0.09	0 %	4.35	9.06	4.71

[a]TSPO Ki values were determined using membrane homogenates of rat heart and screened against [^{3}H]**1** (K_d = 1.8 nM, C = 0.2 nM). [b]*In vitro* binding affinity values are the mean ± SE of duplicate measurements. [c]CBR binding affinity was evaluated using homogenates of rat cerebral cortex and expressed as % of inhibition at 1 μM against [^{3}H]flunitrazepam. [d]Retention time recorded for the tested compounds were converted into their $logD_{7.4}$ values using a validated, standardized HPLC method. [e]LipE values were calculated as follows : LipE = pIC_{50} – $LogD_{7.4}$.

All analogues displayed subnanomolar affinity for the TSPO (0.37 to 0.86 nM), comparable to **2** (0.91 nM). In the fluoroalkyl series, the lowest Ki value was obtained for compound **12** (0.37 nM) whereas in the alkynyl series, it was found for compound **23** (0.35 nM). Additionally, all compounds showed excellent selectivity towards TSPO, except compounds **29** and **30** that both exhibited a slight

binding affinity for the CBR (3 and 12 % at 1 μM, respectively). The $LogD_{7.4}$ values were all higher (3.51 – 4.70) than that of **2** (2.89), most likely due to the replacement of the oxygen atom attached to the phenyl ring, with alkyl- or alkynyl- fragments leading to less hydrophilic structures. These $LogD_{7.4}$ values followed the expected trend of increase with the length of the carbonated side-chain in both series. Nevertheless, most of the $LogD_{7.4}$ values keep in the range for expected good passive cerebral penetration of the ligands. Calculated LipE scores ranged from 4.60 (compound **30**) to 6.11 (compound **2**). The highest LipE score was obtained with **2** and is due to the combination of a subnanomolar affinity for the TSPO and a rather low $logD_{7.4}$ value slightly inferior to 3. Compound **12** also displays a high LipE score of 5.88, while the lengthening of the side chain, especially in the fluoroalkyl- series, resulted in a drop of LipE values below 5 for compounds **29**, **30** and **24**. In the fluoroalkynyl- series, except for compound **24**, LipE values were all comparable (5.35 to 5.61). In particular, despite a $LogD_{7.4}$ value above 4 (4.06), compound **23** exhibited a rather good LipE score (5.35) due to a high TSPO binding affinity. A LipE plot of the binding and lipophilicity data of the compounds is presented in Figure 4.

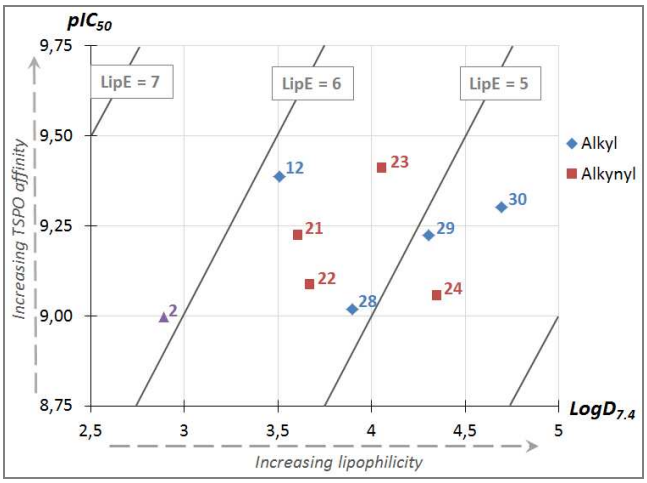

Figure 4. LipE plot of the newly synthesised compounds (**12**, **21**–**24**, **28**–**30**) and **2**: pIC_{50} vs $LogD_{7.4}$.

***In vitro* metabolism.** Oxidative metabolism of **2** and the newly synthesised compounds (**12**, **21**-**24** and **28**-**30**) was investigated using hepatic microsomes from human, rat and mouse. The results, expressed as the percentage of biotransformation obtained after 20 minutes of microsomal incubation, are summarised in Table 2. All compounds are rapidly and extensively metabolised in presence of rat and mouse microsomes, more than 90 % of biotransformation is generally observed after 20 minutes. Biotransformation using human microsomes is more variable, with percentage ranging from 31 % for **2** to 91 % for compound **29**. It can be noted that alkynyl derivatives are less metabolised compared to their alkyl counterparts. These rather pronounced rates of biotransformation are in line with what has already been observed with the parent molecule [^{18}F]**2**:[49] indeed, it has been shown that it is rapidly and extensively metabolised *in vitro* but also *in vivo* in both rodents (rats) and non-human primates (baboons). Identification of the metabolites of **2** and [^{18}F]**2**[49] notably revealed that oxidation reactions occurred mainly (i) at the sensitive methyl positions of the pyrazolo[1,5-*a*]pyrimidine core, (ii) at the alpha-position of the nitrogen atom of the acetamide function leading to *N*-dealkylation and, in a lesser extent, (iii) at the alpha position of the oxygen atom of the fluoroethoxy moiety of **2** leading to the release of fluoroacetate. These oxidative pathways generated hydrophilic species, mainly non-brain penetrant except for [^{18}F]fluoroacetate that cross the BBB and might alter the PET image quality. Contrary to **2**, the newly synthesised compounds (**12**, **21**–**24** and **28**–**30**) don't feature the sensitive ether linkage bridging the fluorine atom to the DPA scaffold and therefore their metabolism may not lead to the unwanted liberation of fluoroacetate. Nevertheless, they still feature the same DPA scaffold and may thus be subjected to a similar oxidative metabolic pathway with regard to oxidation at the methyl positions and *N*-deethylation (or a combination of both). Overall, this *in vitro* study suggests that **2**, **23** and **24** are the less sensitive compounds to

microsomal metabolism, especially with the human subcellular fractions (biotransformation at 20 min < 50 %). And, more specifically, in the fluoroalkyl series, **12** is the less metabolised compound using human microsomes with 79 % biotransformation at 20 minutes compared to 90 ± 1 % for **28**, **29** and **30**.

Table 2. *In vitro* oxidative metabolism.

		% biotransformation at 20 min[a]		
Series	Ligand	*Human*	*Rat*	*Mouse*
	2	31 %	100 %	90 %
Alkyl-	**12**	79 %	100 %	99 %
	28	89 %	99 %	100 %
	29	91 %	99 %	100 %
	30	89 %	97 %	96 %
Alkynyl-	**21**	55 %	99 %	100 %
	22	60 %	98 %	100 %
	23	47 %	91 %	98 %
	24	39 %	96 %	78 %

[a]hepatic microsomal (male CD1 mouse, male Sprague-Dawley rat or humans (BD pool)) incubation, followed by analysis of the supernatant using HPLC/ESI-MS/MS.

On the basis of the *in vitro* preliminary results (affinity, lipophilicity and metabolism) of the newly synthesised compounds: **12**, in the fluoroalkyl series, and **23**, in the fluoroalkynyl series, were chosen for radiolabelling with fluorine-18 to further investigate their *in vivo* PET properties as TSPO radiotracers.

Radiochemistry. Fluorine-18-labelling of compounds **12** and **23** was performed using a TRACERLab FX-FN synthesiser (GEMS) by nucleophilic aliphatic substitution on their corresponding tosylates **31** and **32** (precursors for labelling) with [^{18}F]fluoride (Scheme 3).

Compounds **31** and **32** were synthesised from the corresponding alcohols **11** and **19** by reaction of *p*-toluenesulfonylchloride or *p*-toluenesulfonylanhydride in dichloromethane in presence of triethylamine as depicted in Scheme 3 (85 and 45 % yield, respectively). The efficiency of incorporation of fluorine-18 was first investigated with compound **12** in various reaction conditions and the optimized conditions were then used for the labelling of compound **23** (Table 2). Briefly, the no-carrier-added dried K[^{18}F]F-[2.2.2]-cryptand complex was first prepared from cyclotron-produced [^{18}F]fluoride, potassium carbonate and [2.2.2]-cryptand. An acetonitrile or DMSO solution of the tosylate **31** (or **32**) was then added to the reaction vessel containing K[^{18}F]F-[2.2.2]-cryptand and the resulting mixture was heated at various temperature and for variable duration. The resulting mixture was then diluted with the HPLC mobile phase, pre-purified on a SepPak® Alumina N^{TM} cartridge and purified on an HPLC semi-preparative X-Terra^{TM} RP18 column. Identity of the collected radioactive product was confirmed by co-elution with reference compound **12** (or **23**, respectively) on an analytical HPLC system. Formulated solutions of [^{18}F]**12** (or [^{18}F]**23**), ready for use, were typically obtained after a synthesis time of 50 ± 5 min from end of bombardment (EOB). Average batch product activities, radiochemical yields (RCY) and specific radioactivities (SRA) obtained from the various [^{18}F]**12** radiosynthesis trials are compiled in Table 3.

Scheme 3. Preparation of tosylates 31 and 32, and labelling of [^{18}F]12 and [^{18}F]23*a*.

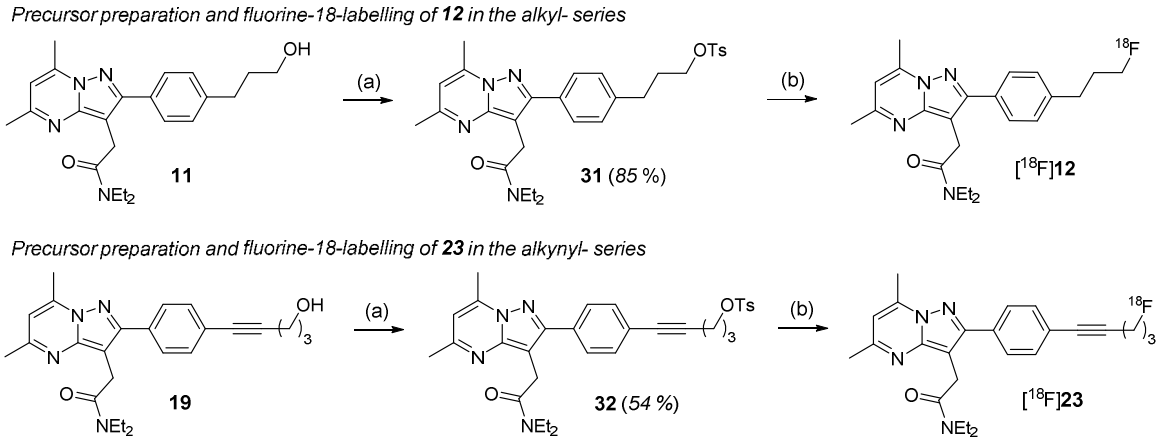

[a]Reaction conditions: (a) TsCl or Ts_2O, TEA, CH_2Cl_2, 0°C to r.t., 5 to 16 h; (b) K[^{18}F]F-[2.2.2]-cryptand, K_2CO_3, solvent, T (°C), time (min) [see Table 3 for details].

Table 3. Labelling conditions and results of radiosynthesis trials for [^{18}F]12 and [^{18}F]23 preparation.

Precursor	Solvent	Temperature (°C)	Reaction time (min)	RCY[a] (d.c.)	SRA[a] (GBq/µmol)	Product
31	DMSO	165	5	38 ± 6	110 ± 5	[^{18}F]**12**
31	CH_3CN	100	10	50 ± 11	75 ± 15	[^{18}F]**12**
31	CH_3CN	100	5	37 ± 10	78 ± 14	[^{18}F]**12**
32	CH_3CN	100	10	24 ± 7	83 ± 9	[^{18}F]**23**

[a]Values are the mean ± SD of at least 3 independent radiosyntheses

Typically, starting from 33–52 GBq of [^{18}F]fluoride, 9–17 GBq of [^{18}F]**12** were obtained, within 50 ± 5 min, with moderate SRA ranging from 60 to 115 GBq/µmol at end of synthesis (EOS). [^{18}F]Fluorination of **12** proved to be the most efficient in acetonitrile when heating the reaction mixture at 100°C for 10 minutes with an average decay-corrected (d.c.) RCY of 50 ± 11%. Attempts to reduce reaction time to 5 min or increase reaction temperature to 165°C in DMSO, led to a lower labelling efficacy with d.c. RCY below 40%. [^{18}F]Fluoride incorporation for the preparation of [^{18}F]**23** was satisfactory using acetonitrile as solvent at 100°C for 10 min and these labelling

conditions were used for the preparation of ready-to-inject [^{18}F]**23** batches for *in vivo* studies. Quality controls were performed on aliquots of formulated radioligands [^{18}F]**12** and [^{18}F]**23**. The radiotracers preparations were clear solutions with a measured pH between 5 and 7. As demonstrated by analytical HPLC analysis, radiochemical and chemical purities were greater than 95 % and the preparations were chemically and radiochemically stable for four hours at ambient temperature on shelve.

Autoradiography. The high binding affinity and selectivity for TSPO of **12** and **23** were confirmed by *in vitro* autoradiography studies of their corresponding radiofluorinated-versions in sections of rat brain with acute local neuroinflammation. Rat brain slices were generated from our in-house model, seven days after an excitotoxic AMPA injection in the right striatum of Wistar rats.[23,34,52] In a first set of experiments, the radioligand was incubated alone and accumulation of the tracer was observed in the lesioned area (right-hand side) when compared to the control side (left-hand side) as seen on Figure 5A for [^{18}F]**12**. In a second and third set of experiments the radioligand was incubated together with an excess of either its non-labelled version (**12** or **23**) or the TSPO ligand of reference **1**. Images obtained either with [^{18}F]**12** (Figure 5B and 5C) or [^{18}F]**23** (not shown here) proved the absence of non-specific binding of the ligands and the specificity for the TSPO target, the binding being fully inhibited in the lesioned area in both cases. Finally, in a fourth set of experiments, the evaluated radioligand was incubated with an excess of flumazenil, a CBR-specific ligand, to confirm its absence of affinity for this target. As shown on Figure 5D and as expected from the previous *in vitro* competition assays with [^{3}H]flunitrazepam (another CBR-specific ligand), the binding of [^{18}F]**12** was not affected by the presence of an excess of flumazenil, proving again its selectivity for the TSPO.

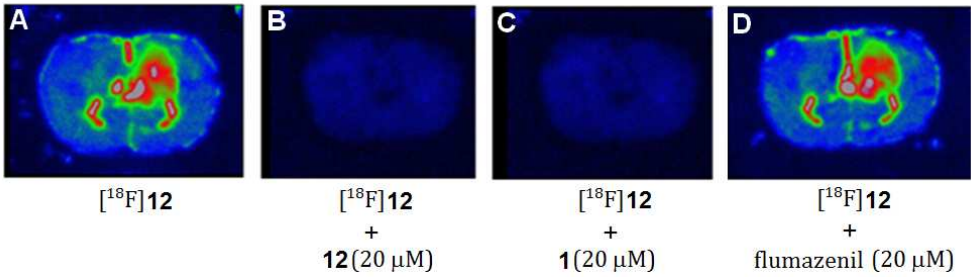

Figure 5. Autoradiography *in vitro* of [^{18}F]**12** (5-10 nM) on rat AMPA-lesioned brain sections : (**A**) alone, (**B**) with non-labelled **12** (20 μM), (**C**) with **1** (20 μM) and (**D**) with flumazenil (20 μM).

Autoradiographic images, obtained with [^{18}F]**23** as radioligand, were comparable to the one presented for [^{18}F]**12**: [^{18}F]**23** accumulates in the lesioned area, and the use of **1** or non-labelled **23** fully inhibited the binding of [^{18}F]**23** while flumazenil did not. The target to background ratio (TBR), calculated as the bound radiotracer in the lesion versus the bound radiotracer in the contralateral side, was determined after incubation of the radiotracer alone and values obtained for [^{18}F]**12** and [^{18}F]**23** are presented in Table 4 for comparison to [^{18}F]**2**. The TBR of [^{18}F]**12** (2.4 ± 0.3) and [^{18}F]**23** (1.9 ± 0.3) were surprisingly more than 50 % lower than the one of [^{18}F]**2** (5.4 ± 2.0).

Table 4. TBR calculated from *in vitro* autoradiographies of [^{18}F]2, [^{18}F]12 and [^{18}F]23.

[^{18}F]-tracer	TBR[a]
[^{18}F]**12**	2.4 ± 0.3
[^{18}F]**23**	1.9 ± 0.3
[^{18}F]**2**	5.4 ± 2.0

[a]TBR values are the mean ± SD of at least 3 independent experiments

Small animal PET studies. PET imaging was performed with [^{18}F]**12** and [^{18}F]**23** on anaesthetised Wistar rats seven days after AMPA-induced brain lesion in the right striatum.[23,34,52] As representative

examples, Figure 6 shows summed coronal, sagittal and axial images of rat brain from 5 to 60 minutes after injection of [^{18}F]**12**. Similar images were obtained after injection of [^{18}F]**23**.

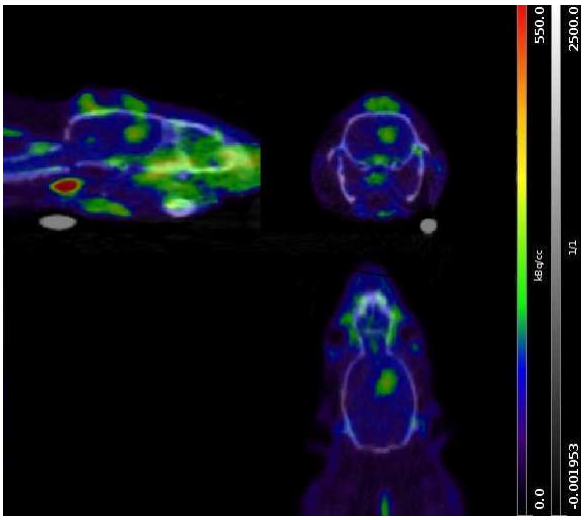

Figure 6. microPET images acquired as summed data from 5 to 60 minutes after intravenous injection of [^{18}F]**12** to AMPA-induced brain lesioned rat.

Data reported in Table 5 show that both [^{18}F]**12** and [^{18}F]**23** rapidly enter the brain with initial uptake values, 2 minutes p.i., in the lesioned striatum of 0.43 and 0.39 percentages of injected dose per milliliter (% ID/mL) respectively. These uptakes were lower 60 minutes p.i. but still relatively high (0.33% for [^{18}F]**12** and 0.24% for [^{18}F]**23**), suggesting that the radiotracers still bound their target. In contrast, uptake in the contralateral side decreased along the study and was rather low 60 minutes p.i. with values of 0.09 and 0.05 % ID/mL for [^{18}F]**12** and [^{18}F]**23**, respectively. A marked contrast between the lesioned area and the corresponding area in the intact contralateral hemisphere of the rat brain was thus obtained for [^{18}F]**12** after 60 minutes, with a calculated ipsilateral-to-contralateral ratio of 3.57 ± 0.48 (n=4) that reflects a high *in vivo* specific binding for the TSPO and is comparable to that measured for [^{18}F]**2** (3.71 ± 0.39). Analogously, the calculated ratio for [^{18}F]**23** reached a

value of 4.62 ± 0.44 (n=4) which is greater than that of [^{18}F]**2**. Noteworthy, these ratios increased along the study and may even be higher using extended imaging protocols. The better contrast obtained with [^{18}F]**23** mainly results from the quicker wash out of the radiotracer in the non-lesioned area. Table 5 compiles the uptake values obtained in the lesioned and non-lesioned area over a period of 60 minutes, as well as the corresponding calculated ipsi/contra ratios for radioligands [^{18}F]**12**, [^{18}F]**23** and [^{18}F]**2**.

Table 5. [^{18}F]12, [^{18}F]23 and [^{18}F]2 uptake values in the lesioned and non-lesioned rat brain areas over a period of 60 minutes post-injection, and the corresponding calculated ipsi/contra ratios.

Time (min)	*Ipsi* uptake (% ID/mL)			*Contra* uptake (% ID/mL)			*Ipsi/contra* ratio		
	[^{18}F]**12**	[^{18}F]**23**	[^{18}F]**2**	[^{18}F]**12**	[^{18}F]**23**	[^{18}F]**2**	[^{18}F]**12**	[^{18}F]**23**	[^{18}F]**2**
2	0.43 ± 0.20	0.39 ± 0.07	0.40 ± 0.02	0.28 ± 0.13	0.23 ± 0.04	0.24 ± 0.02	1.53 ± 0.16	1.70 ± 0.12	1.63 ± 0.12
5	0.40 ± 0.17	0.38 ± 0.05	0.36 ± 0.01	0.23 ± 0.11	0.16 ± 0.03	0.19 ± 0.01	1.72 ± 0.35	2.43 ± 0.32	1.91 ± 0.20
15	0.37 ± 0.16	0.30 ± 0.05	0.34 ± 0.03	0.16 ± 0.08	0.09 ± 0.02	0.12 ± 0.02	2.15 ± 0.33	3.38 ± 0.31	2.76 ± 0.14
40	0.32 ± 0.14	0.25 ± 0.06	0.31 ± 0.05	0.10 ± 0.05	0.06 ± 0.01	0.08 ± 0.02	3.05 ± 0.51	4.01 ± 1.05	3.71 ± 0.49
60	0.33 ± 0.15	0.24 ± 0.04	0.30 ± 0.05	0.09 ± 0.04	0.05 ± 0.01	0.08 ± 0.01	3.57 ± 0.48	4.62 ± 0.44	3.71 ± 0.39

■ CONCLUSION

A novel series of 5,7-dimethylpyrazolo[1,5-a]pyrimidin-3-ylacetamides modified at the 4-positon of the phenyl ring were synthesised and *in vitro* evaluated for their potential to bind the TSPO. All newly synthesised compounds showed comparable or higher affinity for the TSPO than the parent molecule **2**, with Ki values in the subnanomolar range. The TSPO/CBR selectivity was also assessed for all compounds and was proved to be conserved. Determination of their $LogD_{7.4}$ demonstrated moderately increased lipophilicity compared to **2**, however most of the values were in the range for

suitable blood brain barrier passive penetration. Preliminary metabolism studies were also conducted for the title compounds. Among them, two candidates were radiolabelled with fluorine-18 and evaluated *in vitro* and *in vivo* for their specific binding to the TSPO and their potential as PET probes on a rat model of acute neuroinflammation. The data obtained revealed that the newly developed radioligands, [^{18}F]**12** and [^{18}F]**23**, are well suited for imaging neuroinflammation *in vivo*. The potential of these promising PET radiotracers will be further investigated, in particular with regard to their metabolic profiling *in vivo*.

■ EXPERIMENTAL SECTION

General. Chemicals were purchased from Aldrich France and were used without further purification. Flash chromatographies were conducted on silica gel or alumina gel (0.63-0.200 mm, VWR) columns. TLCs were run on pre-coated plates of silica gel $60F_{254}$ (VWR, France). The compounds were localized at 254 nm using a UV-lamp and by dipping the TLC-plates in a 1% ethanolic ninhydrin solution or a basic potassium permanganate aqueous solution and heating on a hot plate.

^{1}H and ^{13}C NMR spectra were recorded on a Bruker (Wissembourg, France) Avance 400 MHz apparatus and chemical shifts were referenced to the hydrogenated residue of the deutereted solvent ($\delta[CD_2HCN]$ = 1.94 ppm, $\delta[CD_2HOD]$ = 3.31 ppm, $\delta[CDHCl_2]$ = 5.32 ppm, $\delta[CHCl_3]$ = 7.24 ppm) for ^{1}H NMR and to the deuterated solvent ($\delta[CD_3CN]$ = 118.7 ppm, $\delta[CD_3OD]$ = 49.2 ppm, $\delta[CD_2Cl_2]$ = 54.0 ppm and $\delta[CDCl_3]$ = 77.2 ppm) for ^{13}C NMR experiments. The standard concentration of the analysed samples was 20 mg/mL. The chemical shifts are reported in ppm, downfield from TMS (s, d, t, q, m and b for singlet, doublet, triplet, quadruplet, multiplet and broad, respectively). The low-resolution mass spectra (MS) were measured on a Thermo Electron (Les Ulis,

France) Ion Trap LCQ Deca XP1 spectrometer (positive electrospray ionization (ESI)). The high-resolution mass spectrometry (HRMS) analyses were performed by Imagif (ICSN-CNRS, Gif-sur-Yvette, France) by electrospray with positive (ESI+) or negative (ESI-) ionization mode. Purity of the synthesised compounds was determined using analytical HPLC (HPLC A) and was found to be more than 95 %. HPLC A: UPLC/SQD Acquity Waters, Acquity BEH C18 (2.1 x 50 mm) column, 1.7 µm, mobile phase: H_2O (A), CH_3CN + 0.1 % formic acid (B), linear gradient from 2 to 100 % (B) in 3 min with a flow rate of 1.0 mL/min. $LogD_{7.4}$ values were determined based on a validated and standardized HPLC method (HPLC B): Alliance 2695 - PDA Waters, X-Terra MS C18 (4.6 x 20 mm, 3.5 µm) column, mobile phase: 5 mM MOPS/$(CH_3)_4NOH$ pH 7.4 (A), 5 % MOPS/$(CH_3)_4NOH$ (100 mM, pH 7.4) / 95 % CH_3CN (B), gradient (A / B): 98:2 (0.5 min), 0:100 (4.8 min), 98:2 (1.6 min), with a flow rate of 1.2 mL/min, 25 °C, detection at 254 nm.

Chemistry. Methyl 4-(3-iodopropoxy)benzoate (3). To a suspension of 18.7 g of potassium carbonate (136 mmol) in acetone (1 L) was added diiodopropane (22.4 mL, 195 mmol). The mixture was stirred at ambient temperature under argon before addition of a solution of 10.0 g of methyl 4-hydroxybenzoate (65.8 mmol) in acetone (100 mL). The reaction mixture was then heated to 50 °C and stirring was prolonged for 16 h. The resulting mixture was filtered to remove insoluble potassium carbonate and the filtrate was evaporated under reduced pressure. The crude product was purified by silica gel column chromatography using heptane/EtOAc (5/1, v/v) as eluent to yield compound **3** (15.2 g, 47.6 mmol, 72 % yield) as light yellow crystals. R_f (heptane/EtOAc: 2/1 v/v): 0.48. ^1H NMR ($CDCl_3$) δ 7.97 (d, J = 8.8 Hz, 2H), 6.91 (d, J = 8.8 Hz, 2H), 4.07 (t, J = 6.2 Hz, 2H), 3.87 (s, 3H), 3.36 (t, J = 6.2 Hz, 2H), 2.28 (q, J = 6.2 Hz, 2H). ^{13}C NMR ($CDCl_3$) δ 166.9 [C], 162.4 [C], 131.7 [2×CH], 122.8 [C], 114.1 [2×CH], 67.4 [CH_2], 51.9 [CH_3], 32.8 [CH_2], 2.2 [CH_2I]. Mp: 47-48°C. ESI(+)-MS: m/z 321 $[M+H]^+$.

Methyl 4-(3-bromopropoxy)benzoate (4). For the preparation of methyl 4-(3-bromopropoxy)benzoate **4**, the procedure described above with methyl 4-hydroxybenzoate **2** was reproduced with dibromopropane instead of diiodopropane as alkylating agent. Starting from 10.0 g of **2** (65.8 mmol), 14.9 g of compound **4** (54.7 mmol, 83 % yield) could be obtained as a white solid after silica gel column chromatography using pure toluene as eluent. R_f (toluene 100 %): 0.32. ^{1}H NMR ($CDCl_3$) δ 7.98 (d, J = 8.8 Hz, 2H), 6.92 (d, J = 8.8 Hz, 2H), 4.16 (t, J = 6.0 Hz, 2H), 3.88 (s, 3H), 3.60 (t, J = 6.4 Hz, 2H), 2.34 (m, 2H). ^{13}C NMR ($CDCl_3$) δ 166.9 [C], 162.5 [C], 131.7 [2×CH], 122.9 [C], 114.2 [2×CH], 65.6 [CH_2], 51.9 [CH_3], 32.2 [CH_2], 29.7 [CH_2]. ESI(+)-MS: m/z, not seen.

Methyl 4-(3-hydroxypropyl)benzoate (5). *Starting from methyl 4-(3-bromopropoxy)benzoate (4):* 12.73 g of **4** (46.6 mmol) were dissolved in dry toluene (1 L) and the solution was stirred under argon and heated to 100 °C. A solution containing azobisisobutyronitrile (AIBN, 1.54 g, 9.4 mmol) and tributyltin hydride (15 mL, 55.9 mmol) in dry toluene (100 mL) was slowly added to the solution of **4** over a period of 1 h and stirring was prolonged at 100 °C overnight. Full conversion of the starting material was confirmed by TLC and the reaction mixture was then concentrated under reduced pressure. The residue was purified by silica gel column chromatography using heptane/EtOAc (2/1, v/v) as eluent to yield compound **5** (1.61 g, 8.30 mmol, 18 % yield) as a light yellow oil.

*Starting from methyl 4-(3-iodopropoxy)benzoate (**3**):*15.2 g of **3** were subjected to the procedure described above. Purification of the crude product afforded compound **5** (1.13 g, 5.82 mmol, 13 % yield). R_f (heptane/EtOAc: 2/1 v/v): 0.14. ^{1}H NMR ($CDCl_3$) δ 7.95 (d, J = 8.4 Hz, 2H), 7.26 (d, J = 8.4 Hz, 2H), 3.90 (s, 3H), 3.67 (t, J = 6.4 Hz, 2H), 2.76 (t, J = 7.6 Hz, 2H), 1.90 (m, 2H). ^{13}C NMR ($CDCl_3$) δ 167.4 [C], 147.6 [C], 129.9 [2×CH], 128.7 [2×CH], 128.1 [C], 62.2 [CH_2], 52.2 [CH_3], 34.0 [CH_2], 32.3 [CH_2]. ESI(+)-MS: m/z, not seen.

Methyl 4-(3-((*tert*-butyldiphenylsilyl)oxy)propyl)benzoate (6). To 1.31 g of **5** (6.75 mmol) dissolved in dry pyridine (25 mL) was added *tert*-butyl-diphenylsilyl chloride (2.11 mL, 8.10 mmol) and the reaction mixture was stirred for 4 h at ambient temperature. After addition of ethyl acetate (200 mL) the solution was washed twice with a 1.0 M aqueous hydrochloric acid solution (2 x 300 mL) and once with brine (250 mL). The organic layer was then dried over sodium sulfate before being filtered and evaporated to dryness. The resulting residue was purified by silica gel column chromatography using toluene/heptane (2/1, v/v) as eluent to yield compound **6** (2.34 g, 5.40 mmol, 80% yield) as a colorless oil. R_f (toluene 100 %): 0.36. ^{1}H NMR ($CDCl_3$) δ 7.93 (d, J = 8.0 Hz, 2H), 7.66 (d, J = 6.4 Hz, 4H), 7.43-7.38 (m, 6H), 7.22 (d, J = 8.0 Hz, 2H), 3.91 (s, 3H), 3.68 (t, J = 6.4 Hz, 2H), 2.79 (t, J = 7.6 Hz, 2H), 1.88 (m, 2H), 1.07 (s, 9H). ^{13}C NMR ($CDCl_3$) δ 167.2 [C], 147.8 [C], 135.6 [4×CH], 133.9 [2×C], 129.7 [2×CH], 129.6 [2×CH], 128.5 [2×CH], 127.7 [C], 127.6 [4×CH], 62.9 [CH_2], 52.0 [CH_3], 33.8 [CH_2], 32.2 [CH_2], 26.9 [3×CH_3], 19.3 [C]. ESI(+)-MS: m/z 433 $[M+H]^+$.

3-(4-(3-((*tert*-Butyldiphenylsilyl)oxy)propyl)phenyl)-3-oxopropanenitrile (7). Sodium methoxide (250 mg, 4.62 mmol), **6** (2.00 g, 4.62 mmol) and dry acetonitrile (25 mL) were mixed at ambient temperature and the resulting reaction mixture was stirred and heated to reflux until the reaction was complete (1-2 days, TLC monitoring). Addition of water (5 mL) and diethyl ether (5 mL) to the mixture allowed extraction in the organic layer of unreacted starting material. The aqueous phase was collected and acidified to pH 6 with 20% aqueous sulfuric acid solution to precipitate the desired compound **7** that was filtered off and dried under vacuum. Compound **7** (695 mg, 1.57 mmol, 34% yield) was obtained as a white powder in a sufficient pure form to be used in the next step without further purification. R_f (toluene/AcOEt 95/5, v/v): 0.33. ^{1}H NMR ($CDCl_3$) δ 7.81 (d, J = 8.0 Hz, 2H), 7.65 (m, 4H), 7.46-7.36 (m, 6H), 7.30 (d, J = 8.0 Hz, 2H), 4.05 (s, 2H), 3.68

(t, J = 6.0 Hz, 2H), 2.81 (t, J = 7.6 Hz, 2H), 1.88 (m, 2H), 1.07 (s, 9H). ^{13}C NMR ($CDCl_3$) δ 186.5 [C], 150.2 [C], 135.5 [4×CH], 133.7 [2×C], 132.0 [C], 129.6 [2×CH], 129.2 [2×CH], 128.5 [2×CH], 127.6 [4×CH], 113.8 [C], 62.6 [CH_2], 33.5 [CH_2], 32.2 [CH_2], 29.2 [CH_2], 26.8 [3×CH_3], 19.2 [C]. ESI(-)-MS: m/z 440 $[M-H]^-$. HR-ESI(+)-MS m/z calcd for $C_{28}H_{30}NO_2Si$: 440.2046 $[M+H]^+$, found 440.2042.

4-(4-(3-((*tert*-Butyldiphenylsilyl)oxy)propyl)phenyl)-3-cyano-*N*,*N*-diethyl-4-oxobutanamide (8). To 16.3 mL of a 0.125 M solution (2.04 mmol) of sodium hydroxide in a 8/2 mixture of ethanol and water, were successively added **7** (750 mg, 1.70 mmol), sodium iodide (765 mg, 5.10 mmol) and *N*,*N*-diethylchloroacetamide (256 μL, 1.87 mmol). The resulting mixture was stirred at 75 °C for 12 h, diluted then with a 0.1 M aqueous hydrochloric acid solution (100 mL) and extracted with ethyl acetate (100 mL). The organic layer was separated, washed with brine, dried over sodium sulfate before being filtered and evaporated to dryness. The resulting residue was purified by silica gel column chromatography using toluene/EtOAc (95/5, v/v) as eluent to yield compound **8** (764 mg, 1.38 mmol, 81 % yield) as an orange oil. R_f (toluene/AcOEt 9/1, v/v): 0.29. ^{1}H NMR (CD_2Cl_2) δ 7.97 (d, J = 8.0 Hz, 2H), 7.70 (m, 4H), 7.45-7.35 (m, 8H), 7.25 (m, 1H), 7.19 (m, 1H), 5.00 (dd, J = 8.8, J = 4.8 Hz, 1H), 3.73 (t, J = 6.0 Hz, 2H), 3.40-3.23 (m, 5H), 2.93 (dd, J = 16.0, J = 4.8 Hz, 1H), 2.86 (t, J = 7.6 Hz, 2H), 1.92 (m, 2H), 1.25 (t, J = 7.2 Hz, 3H), 1.08 (m, 12H). ^{13}C NMR (CD_2Cl_2) δ 189.5 [C], 166.8 [C], 149.9 [C], 135.4 [4×CH], 133.8 [2×C], 132.0 [C], 129.5 [2×CH], 129.1 [2×CH], 128.9 [2×CH], 127.6 [4×CH], 117.4 [C], 62.7 [CH_2], 41.8 [CH_2], 40.4 [CH_2], 34.0 [CH], 33.6 [CH_2], 32.9 [CH_2], 32.1 [CH_2], 26.5 [3×CH_3], 19.0 [C], 13.8 [CH_3], 12.6 [CH_3]. ESI(+)-MS: m/z 555 $[M+H]^+$, 577 $[M+Na]^+$, 593 $[M+K]^+$. HR-ESI(+)-MS m/z calcd for $C_{34}H_{43}N_2O_3Si$: 555.3043 $[M+H]^+$, found 555.3036.

2-(3-Amino-5-(4-(3-((*tert*-butyldiphenylsilyl)oxy)propyl)phenyl)-1*H*-pyrazol-4-yl)-*N*,*N*-diethylacetamide (9). To 750 mg of **8** (1.35 mmol) dissolved in ethanol (6.8 mL) were added glacial acetic acid (140 µL) and hydrazine monohydrate (100 µL, 2.03 mmol). The resulting reaction mixture was stirred at 60 °C for 3 h, cooled down to room temperature and diluted with ethyl acetate (100 mL). The organic layer was successively washed with a saturated aqueous ammonium chloride solution, brine and dried over sodium sulfate before being filtered and evaporated to dryness. The resulting residue was purified by silica gel column chromatography using CH_2Cl_2/MeOH (9/1, v/v) as eluent to yield compound **9** (734 mg, 1.29 mmol, 95 % yield) as a light pink oil. R_f (CH_2Cl_2/MeOH 95/5, v/v): 0.15. ^{1}H NMR (CD_2Cl_2) δ 7.68 (m, 4H), 7.46-7.38 (m, 6H), 7.32-7.26 (m, 4H), 3.72 (t, J = 6.0 Hz, 2H), 3.49 (s, 2H), 3.32 (q, J = 7.2 Hz, 2H), 3.07 (q, J = 7.2 Hz, 2H), 2.80 (t, J = 7.6 Hz, 2H), 1.91 (m, 2H), 1.09 (m, 12H), 0.90 (t, J = 7.2 Hz, 3H). ^{13}C NMR (CD_2Cl_2) δ 170.0 [C], 153.5 [C], 142.9 [C], 142.8 [C], 135.4 [4×CH], 134.0 [C], 133.9 [2×C], 129.5 [2×CH], 129.0 [2×CH], 127.6 [4×CH], 127.5 [2×CH], 98.0 [C], 62.9 [CH_2], 42.2 [CH_2], 40.3 [CH_2], 34.0 [CH_2], 31.7 [CH_2], 28.2 [CH_2], 26.5 [3×CH_3], 19.0 [C], 13.8 [CH_3], 12.7 [CH_3]. ESI(+)-MS: m/z 569 $[M+H]^+$, 591 $[M+Na]^+$, 607 $[M+K]^+$.

2-(2-(4-(3-((*tert*-Butyldiphenylsilyl)oxy)propyl)phenyl)-5,7-dimethylpyrazolo[1,5-a]pyrimidin-3-yl)-*N*,*N*-diethylacetamide (10). To 720 mg of **9** (1.27 mmol) dissolved in ethanol (16 mL) was added pentan-2,4-dione (143 µL, 1.39 mmol) and the resulting mixture stirred overnight at 60 °C. Evaporation of the reaction solvent afforded a crude product that was purified by silica gel column chromatography using pure ethyl acetate as eluent to yield compound **10** (600 mg, 0.95 mmol, 75% yield) as a beige powder. R_f (EtOAc 100 %): 0.18. ^{1}H NMR (CD_2Cl_2) δ 7.70 (m, 6H), 7.46-7.38 (m, 6H), 7.29 (d, J = 8.4 Hz, 2H), 6.58 (s, 1H), 3.91 (s, 2H), 3.75 (t, J = 6.0 Hz, 2H), 3.50 (q, J = 7.2 Hz, 2H), 3.40 (q, J = 7.2 Hz, 2H), 2.80 (t, J = 7.6 Hz, 2H), 2.76 (s, 3H), 2.57 (s, 3H), 1.94

(m, 2H), 1.23 (t, J = 7.2 Hz, 3H), 1.12 (t, J = 7.2 Hz, 3H), 1.09 (s, 9H). ^{13}C NMR (CD_2Cl_2) δ 169.6 [C], 157.6 [C], 154.5 [C], 147.6 [C], 144.8 [C], 142.5 [C], 135.5 [4×CH], 133.9 [2×C], 131.3 [C], 129.5 [2×CH], 128.5 [2×CH], 128.2 [2×CH], 127.5 [4×CH], 108.2 [CH], 100.9 [C], 63.0 [CH_2], 42.1 [CH_2], 40.4 [CH_2], 34.1 [CH_2], 31.7 [CH_2], 27.9 [CH_2], 26.6 [3×CH_3], 24.3 [CH_3], 19.0 [C], 16.6 [CH_3], 13.9 [CH_3], 12.8 [CH_3]. ESI(+)-MS: m/z 633 $[M+H]^+$, 655 $[M+Na]^+$, 671 $[M+K]^+$. HR-ESI(+)-MS m/z calcd for $C_{39}H_{49}N_4O_2Si$: 633.3625 $[M+H]^+$, found 633.3607.

N*,*N*-Diethyl-2-(2-(4-(3-hydroxypropyl)phenyl)-5,7-dimethylpyrazolo[1,5-a]pyrimidin-3-yl)acetamide (11).** *From **10: To 585 mg of **10** (0.93 mmol) dissolved in tetrahydrofuran (5 mL), was added tetrabutylammonium fluoride (TBAF, 1.0 M in tetrahydrofuran, 1.85 mL, 1.85 mmol) and the resulting reaction mixture stirred at ambient temperature overnight. The mixture was then diluted with ethyl acetate and successively washed with a saturated aqueous ammonium chloride solution and brine. The organic layer was dried over sodium sulfate, filtered and evaporated to dryness. The resulting residue was purified by silica gel column chromatography using CH_2Cl_2/MeOH (97/3, v/v) as eluent to yield compound **11** (240 mg, 0.61 mmol, 66 % yield) as a white powder.

*From **17***: To a solution of 209 mg of *N*,*N*-diethyl-2-(2-(4-(4-hydroxyprop-1-yn-1-yl)phenyl)-5,7-dimethylpyrazolo[1,5-a]pyrimidin-3-yl)acetamide **17** (0.536 mmol) in dichloromethane (4-5 mL) was added 10 % palladium on charcoal (5 mol %). The reaction flask was degassed under vacuum and filled with hydrogen at 1 atm. and the reaction mixture was stirred at ambient temperature for 24 h. The mixture was then filtered on a silica pad and washed with a mixture of CH_2Cl_2/MeOH (8/2, v/v). The filtrate was concentrated to dryness and the residue was purified by silica gel column chromatography using CH_2Cl_2/MeOH (99/1 to 95/5, v/v) as eluent to afford compound **11** (194 mg, 0.492 mmol, 92 % yield) as a white solid. R_f (CH_2Cl_2/MeOH 95/5, v/v): 0.17. ^{1}H NMR (CD_2Cl_2) δ 7.70 (d, J = 8.0 Hz, 2H), 7.29 (d, J = 8.0 Hz, 2H), 6.56 (s, 1H), 3.89 (s, 2H), 3.63 (t, J = 6.4 Hz, 2H),

3.49 (q, J = 7.2 Hz, 2H), 3.39 (q, J = 7.2 Hz, 2H), 2.73 (m, 5H), 2.53 (s, 3H), 1.87 (m, 2H), 1.70 (bs, 1H), 1.22 (t, J = 7.2 Hz, 3H), 1.10 (t, J = 7.2 Hz, 3H). ^{13}C NMR (CD_2Cl_2) δ 169.6 [C], 157.6 [C], 154.5 [C], 147.6 [C], 144.8 [C], 142.3 [C], 131.4 [C], 128.5 [2×CH], 128.3 [2×CH], 108.2 [CH], 100.9 [C], 61.9 [CH_2], 42.1 [CH_2], 40.4 [CH_2], 34.3 [CH_2], 31.8 [CH_2], 27.9 [CH_2], 24.3 [CH_3], 16.6 [CH_3], 14.0 [CH_3], 12.8 [CH_3]. ESI(+)-MS: m/z 395 $[M+H]^+$, 417 $[M+Na]^+$, 433 $[M+K]^+$. HR-ESI(+)-MS m/z calcd for $C_{23}H_{31}N_4O_2$: 395.2447 $[M+H]^+$, found 395.2447.

***N,N*-Diethyl-2-(2-(4-(3-fluoropropyl)phenyl)-5,7-dimethylpyrazolo[1,5-a]pyrimidin-3-yl)acetamide (12).** 168 mg (0.43 mmol) of *N,N*-diethyl-2-(2-(4-(3-hydroxypropyl)phenyl)-5,7-dimethylpyrazolo[1,5-a]pyrimidin-3-yl)acetamide **11**, were reacted with bis(2-methoxyethyl) aminosulfur trifluoride (Deoxo-Fluor®, 50% solution in toluene, 0.28 mL, 1.07 mmol) in toluene (2.5 mL) at room temperature for 6 h. The reaction mixture was then evaporated to dryness and the residue purified by silica gel column chromatography using CH_2Cl_2/MeOH (99/1, v/v) as eluent to give compound **1** (88 mg, 0.22 mmol, 52 % yield) as a beige solid. R_f (CH_2Cl_2/MeOH 98/2 v/v): 0.50. t_R (HPLC A) = 1.18 min. ^{1}H NMR ($CDCl_3$) δ 7.74 (d, J = 8.0 Hz, 2H), 7.28 (d, J = 8.0 Hz, 2H), 6.52 (s, 1H), 4.46 (dt, J^2_{H-F} = 46.8 Hz, J^3_{H-H} = 6.0 Hz, 2H), 3.93 (s, 2H), 3.49 (q, J = 7.2 Hz, 2H), 3.40 (q, J = 7.2 Hz, 2H), 2.79 (t, J = 7.2 Hz, 2H), 2.74 (s, 3H), 2.54 (s, 3H), 2.10-1.96 (m, 2H), 1.20 (t, J = 7.2 Hz, 3H), 1.10 (t, J = 7.2 Hz, 3H). ^{13}C NMR (CD_2Cl_2) δ 169.6 [C], 157.6 [C], 154.4 [C], 147.6 [C], 144.8 [C], 141.4 [C], 131.7 [C], 128.5 [2×CH], 128.4 [2×CH], 108.2 [CH], 101.0 [C], 83.2 [d, J^1_{C-F} = 163.0 Hz, CH_2F], 42.1 [CH_2], 40.4 [CH_2], 31.9 [d, J^2_{C-F} = 20.0 Hz, CH_2], 31.0 [d, J^3_{C-F} = 6.0 Hz, CH_2], 27.9 [CH_2], 24.3 [CH_3], 16.5 [CH_3], 14.0 [CH_3], 12.8 [CH_3]. ESI(+)-MS: m/z 397 $[M+H]^+$, 419 $[M+Na]^+$. HR-ESI(+)-MS m/z calcd for $C_{23}H_{30}FN_4O$: 397.2404 $[M+H]^+$, found 397.2411.

3-(4-Iodophenyl)-3-oxopropanenitrile (13). To 50 mL of anhydrous tetrahydrofuran cooled at -60 °C was added first a 1.6 M *n*-butyllithium solution in hexanes (62.5 mL, 100 mmol) and then,

cautiously, a solution of acetonitrile (5.2 mL, 100 mmol) in anhydrous tetrahydrofuran (50 mL) over a period of 15-20 min while maintaining the temperature below -50 °C. The mixture was then stirred for 30 min at -60 °C. 12.0 g of methyl 4-iodobenzoate (45.8 mmol) dissolved in anhydrous tetrahydrofuran (70 mL) was then cautiously channeled to the mixture over 20 min while maintaining the temperature below -50 °C. Once the addition finished, the reaction mixture was stirred for 1 h at -60 °C and 2 h at -45 °C. Once completed (TLC-monitoring), the reaction was quenched at -40 °C with addition of water (200 mL) under vigorous stirring. Then, a 37 % aqueous hydrochloric acid solution was added to acidify the aqueous layer to pH 2. A white inorganic precipitate was filtered off and the filtrate was extracted twice with ethyl acetate (2 x 200 mL). The combined organic layers were washed with water (2 x 100 mL) and brine (100 mL), dried over sodium sulfate, filtered and concentrated to dryness to afford pure compound **13** (8.64g, 31.9 mmol, 70 % yield) as a beige solid. R_f (heptane/acetone 3/1, v/v): 0.28. ^{1}H NMR (CD_3CN) δ 7.95 (d, J = 8.4 Hz, 2H), 7.64 (d, J = 8.4 Hz, 2H), 4.29 (s, 2H). ^{13}C NMR (CD_3CN) δ 188.5 [C], 138.2 [2xCH], 134.1 [C], 129.7 [2xCH], 114.6 [C], 101.8 [C], 29.7 [CH_2]. ESI(-)-MS: m/z 270 $[M-H]^-$. HR-ESI(-)-MS *m/z* calcd for C_9H_5NOI: 269.9416 $[M-H]^-$, found 269.9421.

3-Cyano-*N*,*N*-diethyl-4-(4-iodophenyl)-4-oxobutanamide (14). To a solution containing 8.64 g of **13** (31.9 mmol) in a mixture of ethanol (170 mL) and water (30 mL) was added portionwise and under vigorous stirring sodium hydroxide (1.40 g, 35.0 mmol). The reaction mixture was stirred for 15 min at ambient temperature and then sodium iodide (9.60 g, 64.0 mmol) was added in one portion, followed by the dropwise addition of *N,N*-diethylchloroacetamide (4.40 mL, 32.1 mmol). The reaction mixture was stirred for 4 days at ambient temperature. Once the reaction completed (TLC-monitoring), the suspension was filtered to remove inorganic salt and the filtrate was concentrated to dryness. The residue was was purified by silica gel column chromatography using CH_2Cl_2/MeOH (100/0 to 98/2, v/v) as eluent to yield compound **14** (6.61 g, 17.2 mmol, 54 % yield) as a beige

powder. R_f (heptane/EtOAc 2/1, v/v): 0.26. ^{1}H NMR ($CDCl_3$) δ 7.76 (d, J = 8.0 Hz, 2H), 7.60 (d, J = 8.0 Hz, 2H), 4.95 (dd, J = 9.6 Hz, J = 4.0 Hz, 1H), 3.50-3.25 (m, 5H), 2.88 (dd, J = 12.0 Hz, J = 4.0 Hz, 1H), 1.27 (t, J = 7.0 Hz, 3H), 1.10 (t, J = 7.0 Hz, 3H). ^{13}C NMR ($CDCl_3$) δ 189.1 [C], 166.8 [C], 138.4 [2xCH], 133.6 [C], 130.1 [2xCH], 116.7 [C], 102.8 [C], 42.0 [CH_2], 40.6 [CH_2], 33.7 [CH], 32.7 [CH_2], 14.0 [CH_3], 12.9 [CH_3]. ESI(-)-MS: m/z 383 $[M-H]^-$. HR-(ESI+)-MS *m/z* calcd for $C_{15}H_{18}IN_2O_2$: 385.0413 $[M+H]^+$, found 385.0428.

2-(3-Amino-5-(4-iodophenyl)-1*H*-pyrazol-4-yl)-*N*,*N*-diethylacetamide (15). To 2.25 g of **14** (5.86 mmol) dissolved in ethanol (30 mL) was added monohydrated hydrazine (802 µL, 16.4 mmol) and glacial acetic acid (586 µL, 10.2 mmol). The reaction mixture was heated at 80 °C for 3 h and then concentrated to dryness. The residue was partitioned between water (50 mL), which was basified at pH 10 with a 3.0 M sodium hydroxide aqueous solution, and ethyl acetate (50 mL). The organic layer was separated, washed with water (2 x 50 mL) and brine (50 mL), dried over sodium sulfate, filtered and concentrated to dryness. The residue was triturated in cold diethyl ether (10 mL) to give a solid which was collected, washed with cold diethyl ether (2 x 5 mL) and suck-dried to afford pure compound **15** (1.80 g, 4.52 mmol, 77 % yield) as a beige powder. R_f (CH_2Cl_2/MeOH 93/7, v/v): 0.20. ^{1}H NMR (CD_3OD) δ 7.78 (d, J = 8.4 Hz, 2H), 7.22 (d, J = 8.4 Hz, 2H), 3.54 (s, 2H), 3.31 (q, J = 7.2 Hz, 2H), 3.24 (q, J = 7.2 Hz, 2H), 1.06 (t, J = 7.2 Hz, 3H), 1.00 (t, J = 7.2 Hz, 3H). ^{13}C NMR (CD_3OD) δ 170.9 [C], 152.5 [C], 143.0 [C], 137.6 [2xCH], 131.0 [C], 129.2 [2xCH], 97.0 [C], 93.0 [C], 42.1 [CH_2], 40.4 [CH_2], 27.8 [CH_2], 12.7 [CH_3], 11.7 [CH_3]. ESI(+)-MS: m/z 399 $[M+H]^+$. HR-(ESI+)-MS *m/z* calcd for $C_{15}H_{20}IN_4O$: 399.0682 $[M+H]^+$, found 399.0674.

***N*,*N*-Diethyl-2-(2-(4-iodophenyl)-5,7-dimethylpyrazolo[1,5-a]pyrimidin-3-yl)acetamide (16).** To a solution of 7.0 g of **15** (17.6 mmol) in ethanol (140 mL) was added acetylacetone (2.9 mL, 28.2 mmol). The reaction mixture was heated to reflux for 5 h and was left cooled down to ambient temperature without stirring overnight allowing the product to crystallize spontaneously. The crystals

were filtered, washed with cold ethanol (2 x 20 mL) and suck-dried under vacuum to afford pure compound **16** (6.4 g, 13.8 mmol, 78 % yield) as white needles. R_f (CH_2Cl_2/acetone 8/2, v/v): 0.48. ^{1}H NMR ($CDCl_3$) δ 7.77 (d, J = 8.4 Hz, 2H), 7.60 (d, J = 8.4 Hz, 2H), 6.54 (s, 1H), 3.95 (s, 2H), 3.52 (q, J = 7.2 Hz, 2H), 3.40 (q, J = 7.2 Hz, 2H), 2.74 (s, 3H), 2.57 (s, 3H), 1.23 (t, J = 7.2 Hz, 3H), 1.11 (t, J = 7.2 Hz, 3H). ^{13}C NMR ($CDCl_3$) δ 169.8 [C], 157.7 [C], 154.0 [C], 147.6 [C], 144.7 [C], 137.5 [2xCH], 133.3 [C], 130.4 [2xCH], 108.5 [CH], 101.2 [C], 94.4 [C], 42.3 [CH_2], 40.6 [CH_2], 27.9 [CH_2], 24.6 [CH_3], 16.8 [CH_3], 14.3 [CH_3], 13.0 [CH_3]. HR-(ESI+)-MS *m/z* calcd for $C_{20}H_{24}IN_4O$: 463.0995 $[M+H]^+$, found 463.1011.

General procedure for the synthesis of *N*,*N*-diethyl-2-(2-(4-(*n*-hydroxyalk-1-yn-1-yl)phenyl)-5,7-dimethylpyrazolo[1,5-a]pyrimidin-3-yl)acetamide (17-20). To 200 mg of **16** (0.432 mmol) dissolved in triethylamine (4 mL) was added, under argon, the appropriate alkynol (1.2 eq), followed by palladium bis(triphenylphosphine)dichloride (2 mg, 0.5 mol %) and copper iodide (1 mg, 0.01 eq). The reaction mixture was stirred at ambient temperature for 48 h and concentrated to dryness. The resulting residue was partitioned between ethyl acetate (20 mL) and water (20 mL). The organic layer was collected and the aqueous layer was extracted once again with ethyl acetate (20 mL). The organic layers were combined, washed with brine (30 mL), dried over sodium sulfate, filtered and concentrated to dryness. The residue was purified by silica gel column chromatography using CH_2Cl_2/MeOH (99/1 to 95/5, v/v) as eluent to afford the title compounds.

***N*,*N*-Diethyl-2-(2-(4-(4-hydroxyprop-1-yn-1-yl)phenyl)-5,7-dimethylpyrazolo[1,5-a]pyrimidin-3-yl)acetamide (17).** The procedure described above was used with prop-2-yn-1-ol (29 mg, 518 mmol) to give compound **17** (108 mg, 0.277 mmol, 64 % yield) as a beige powder. R_f (CH_2Cl_2/MeOH 93/7, v/v): 0.29. ^{1}H NMR ($CDCl_3$) δ 7.79 (d, J = 8.0 Hz, 2H), 7.50 (d, J = 8.0 Hz, 2H), 6.55 (s, 1H), 4.48 (s, 2H), 3.98 (s, 2H), 3.52 (q, J = 7.2 Hz, 2H), 3.40 (q, J = 7.2 Hz, 2H), 2.76

(s, 3H), 2.59 (s, 3H), 1.23 (t, J = 7.2 Hz, 3H), 1.11 (t, J = 7.2 Hz, 3H). ^{13}C NMR ($CDCl_3$) δ 169.9 [C], 157.7 [C], 154.2 [C], 147.5 [C], 144.8 [C], 133.8 [C], 131.7 [2xCH], 128.4 [2xCH], 122.4 [C], 108.5 [CH], 101.3 [C], 88.1 [C], 85.4 [C], 51.4 [CH_2], 42.3 [CH_2], 40.6 [CH_2], 27.9 [CH_2], 24.5 [CH_3], 16.8 [CH_3], 14.3 [CH_3], 13.0 [CH_3]. HR-(ESI+)-MS *m/z* calcd for $C_{23}H_{27}N_4O_2$: 391.2134 $[M+H]^+$, found 391.2137.

***N*,*N*-Diethyl-2-(2-(4-(4-hydroxybut-1-yn-1-yl)phenyl)-5,7-dimethylpyrazolo[1,5-a]pyrimidin-3-yl)acetamide (18).** The procedure described above was used with but-3-yn-1-ol (36 mg, 518 mmol) to give compound **18** (136 mg, 0.336 mmol, 78 % yield) as beige crystals. R_f (CH_2Cl_2/MeOH 95/5, v/v): 0.22. ^{1}H NMR ($CDCl_3$) δ 7.77 (d, J = 8.0 Hz, 2H), 7.48 (d, J = 8.0 Hz, 2H), 6.53 (s, 1H), 3.91 (s, 2H), 3.80 (t, J = 6.4 Hz, 2H), 3.50 (q, J = 7.2 Hz, 2H), 3.40 (q, J = 7.2 Hz, 2H), 2.73 (s, 3H), 2.69 (t, J = 6.4 Hz, 2H), 2.54 (s, 3H), 1.20 (t, J = 7.2 Hz, 3H), 1.10 (t, J = 7.2 Hz, 3H). ^{13}C NMR ($CDCl_3$) δ 169.9 [C], 157.7 [C], 154.3 [C], 147.7 [C], 144.7 [C], 133.3 [C], 131.7 [2xCH], 128.4 [2xCH], 123.2 [C], 108.5 [CH], 101.2 [C], 87.2 [C], 82.3 [C], 61.0 [CH_2], 42.3 [CH_2], 40.6 [CH_2], 27.9 [CH_2], 24.6 [CH_3], 23.8 [CH_2], 16.8 [CH_3], 14.3 [CH_3], 13.0 [CH_3]. HR-(ESI+)-MS *m/z* calcd for $C_{24}H_{29}N_4O_2$: 405.2291 $[M+H]^+$, found 405.2303.

***N*,*N*-Diethyl-2-(2-(4-(4-hydroxypent-1-yn-1-yl)phenyl)-5,7-dimethylpyrazolo[1,5-a]pyrimidin-3-yl)acetamide (19).** The procedure described above was used with pent-4-yn-1-ol (44 mg, 518 mmol) to give compound **19** (125 mg, 0.298 mmol, 69 % yield) as a white solid. R_f (CH_2Cl_2/MeOH 94/6, v/v): 0.39. ^{1}H NMR ($CDCl_3$) δ 7.74 (d, J = 8.0 Hz, 2H), 7.46 (d, J = 8.0 Hz, 2H), 6.54 (s, 1H), 3.93 (s, 2H), 3.81 (t, J = 6.4 Hz, 2H), 3.49 (q, J = 7.2 Hz, 2H), 3.40 (q, J = 7.2 Hz, 2H), 2.74 (s, 3H), 2.56 (s, 3H), 2.55 (t, J = 6.4 Hz, 2H), 1.86 (q^5, J = 6.4 Hz, 2H), 1.22 (t, J = 7.2 Hz, 3H), 1.10 (t, J = 7.2 Hz, 3H). ^{13}C NMR ($CDCl_3$) δ 169.8 [C], 157.6 [C], 154.5 [C], 147.5 [C], 145.0 [C], 133.0 [C], 131.6 [2xCH], 128.4 [2xCH], 123.6 [C], 108.4 [CH], 101.3 [C], 90.2 [C], 81.1 [C],

61.7 [CH_2], 42.2 [CH_2], 40.6 [CH_2], 31.3 [CH_2], 28.0 [CH_2], 24.5 [CH_3], 16.8 [CH_3], 16.0 [CH_2], 14.3 [CH_3], 13.0 [CH_3]. HR-(ESI+)-MS *m/z* calcd for $C_{25}H_{31}N_4O_2$: 419.2447 $[M+H]^+$, found 419.2460.

***N,N*-Diethyl-2-(2-(4-(4-hydroxyhex-1-yn-1-yl)phenyl)-5,7-dimethylpyrazolo[1,5-a]pyrimidin-3-yl)acetamide (20).** The procedure described above was used with hex-5-yn-1-ol (51 mg, 518 mmol) to give compound **20** (149 mg, 0.346 mmol, 80 % yield) as beige crystals. R_f (CH_2Cl_2/MeOH 95/5, v/v): 0.23. ^{1}H NMR ($CDCl_3$) δ 7.75 (d, J = 8.0 Hz, 2H), 7.46 (d, J = 8.0 Hz, 2H), 6.52 (s, 1H), 3.94 (s, 2H), 3.69 (t, J = 4.0 Hz, 2H), 3.49 (q, J = 7.2 Hz, 2H), 3.40 (q, J = 7.2 Hz, 2H), 2.74 (s, 3H), 2.55 (s, 3H), 2.46 (t, J = 6.8 Hz, 2H), 1.81-1.65 (m, 4H), 1.23 (t, J = 7.2 Hz, 3H), 1.10 (t, J = 7.2 Hz, 3H). ^{13}C NMR ($CDCl_3$) δ 169.7 [C], 157.6 [C], 154.5 [C], 147.5 [C], 145.0 [C], 132.8 [C], 131.6 [2xCH], 128.4 [2xCH], 123.8 [C], 108.4 [CH], 101.3 [C], 90.7 [C], 80.9 [C], 62.3 [CH_2], 42.2 [CH_2], 40.6 [CH_2], 31.8 [CH_2], 28.0 [CH_2], 24.9 [CH_2], 24.3 [CH_3], 19.2 [CH_2], 16.9 [CH_3], 14.3 [CH_3], 13.0 [CH_3]. HR-(ESI+)-MS *m/z* calcd for $C_{26}H_{33}N_4O_2$: 433.2604 $[M+H]^+$, found 433.2612.

General procedure for the synthesis of *N,N*-diethyl-2-(2-(4-(*n*-fluoroalk-1-yn-1-yl)phenyl)-5,7-dimethylpyrazolo[1,5-a]pyrimidin-3-yl)acetamide (21-24). To the appropriate *N,N*-diethyl-2-(2-(4-(*n*-hydroxyalk-1-yn-1-yl)phenyl)-5,7-dimethylpyrazolo[1,5-*a*]pyridimin-3-yl)acetamide dissolved in toluene (2-4 mL) and dichloromethane (1.0-2.5 mL), were added 2-3 eq of a 50% Deoxo-Fluor® solution in toluene. The reaction mixture was stirred for 24 to 72 h at ambient temperature and additional Deoxo-Fluor® solution was added if required (TLC monitoring) to complete the conversion of the starting alcohol. The solvent was removed under vacuum and the resulting residue was dissolved in ethyl acetate (20 mL) and successively washed with water (20 mL) and brine (20 mL) before being dried over sodium sulfate, filtered and evaporated to dryness. The

crude material was purified by silica gel column chromatography using CH_2Cl_2/MeOH (99/1 to 95/5, v/v) as eluent to yield the title compounds.

***N*,*N*-Diethyl-2-(2-(4-(3-fluoroprop-1-yn-1-yl)phenyl)-5,7-dimethylpyrazolo[1,5-a]pyrimidin-3-yl)acetamide (21).** Starting from 210 mg (0.538 mmol) of **17** and using the general procedure described above, compound **21** (17 mg, 0.043 mmol, 8 % yield) was isolated as a white powder. R_f (CH_2Cl_2/MeOH 95/5, v/v): 0.42. t_R (HPLC A) = 1.19 min. ^{1}H NMR ($CDCl_3$) δ 7.83 (d, J = 8.0 Hz, 2H), 7.55 (d, J = 8.0 Hz, 2H), 6.55 (s, 1H), 5.20 (d, J^2_{HF} = 47.6 Hz, 2H), 3.95 (s, 2H), 3.52 (q, J = 7.2 Hz, 2H), 3.40 (q, J = 7.2 Hz, 2H), 2.75 (s, 3H), 2.56 (s, 3H), 1.23 (t, J = 7.2 Hz, 3H), 1.11 (t, J = 7.2 Hz, 3H). ^{13}C NMR ($CDCl_3$) δ 169.7 [C], 157.7 [C], 154.2 [C], 147.5 [C], 145.0 [C], 134.4 [C], 131.9 [2xCH], 128.5 [2xCH], 121.5 [d, J^4_{CF} = 4 Hz, C], 108.5 [CH], 101.4 [C], 89.5 [d, J^3_{CF} = 12 Hz, C], 83.2 [d, J^2_{CF} = 22 Hz, C], 71.1 [d, J^1_{CF} = 164 Hz, CH_2], 42.3 [CH_2], 40.6 [CH_2], 27.9 [CH_2], 24.4 [CH_3], 16.8 [CH_3], 14.3 [CH_3], 13.0 [CH_3]. (ESI+)-MS: *m/z* 393 $[M+H]^+$. HR-(ESI+)-MS *m/z* calcd for $C_{23}H_{26}FN_4O$: 393.2090 $[M+H]^+$, found 393.2084.

***N*,*N*-Diethyl-2-(2-(4-(4-fluorobut-1-yn-1-yl)phenyl)-5,7-dimethylpyrazolo[1,5-a]pyrimidin-3-yl)acetamide (22).** Starting from 260 mg (0.643 mmol) of **18** and using the general procedure described above, compound **22** (162 mg, 0.399 mmol, 62 % yield) was isolated as a colorless oil. R_f (CH_2Cl_2/MeOH 93/7, v/v): 0.48. t_R (HPLC A) = 1.20 min. ^{1}H NMR ($CDCl_3$) δ 7.77 (d, J = 8.0 Hz, 2H), 7.48 (d, J = 8.0 Hz, 2H), 6.52 (s, 1H), 4.60 (dt, J^2_{HF} = 46.8 Hz, J^3_{HH} = 6.8 Hz, 2H), 3.94 (s, 2H), 3.50 (q, J = 7.2 Hz, 2H), 3.40 (q, J = 7.2 Hz, 2H), 2.86 (dt, J^3_{HF} = 19.2 Hz, J^3_{HH} = 6.8 Hz, 2H), 2.73 (s, 3H), 2.55 (s, 3H), 1.24 (t, J = 7.2 Hz), 1.11 (t, J = 7.2 Hz, 3H). ^{13}C NMR ($CDCl_3$) δ 169.6 [C], 157.6 [C], 154.0 [C], 147.5 [C], 145.1 [C], 133.2 [C], 131.7 [2xCH], 128.5 [2xCH], 123.1 [C], 108.3 [CH], 101.3 [C], 89.4 [C], 85.1 [d, J^3_{CF} = 6 Hz, C], 81.3 [d, J^1_{CF} = 171 Hz, CH_2], 42.2 [CH_2], 40.6 [CH_2], 28.0 [CH_2], 24.1 [CH_3], 21.6 [d, J^2_{CF} = 24 Hz, CH_2], 16.9 [CH_3], 14.3 [CH_3], 13.0 [CH_3].

(ESI+)-MS: *m/z* 407 $[M+H]^+$. HR-(ESI+)-MS *m/z* calcd for $C_{24}H_{28}FN_4O$: 407.2247 $[M+H]^+$, found 407.2248.

***N*,*N*-Diethyl-2-(2-(4-(5-fluoropent-1-yn-1-yl)phenyl)-5,7-dimethylpyrazolo[1,5-a]pyrimidin-3-yl)acetamide (23).** Starting from 260 mg (0.622 mmol) of **19** and using the general procedure described above, compound **23** (50 mg, 0.118 mmol, 19 % yield) was isolated as a light yellow powder. R_f (CH_2Cl_2/MeOH 93/7, v/v): 0.54. t_R (HPLC A) = 1.30 min. ^{1}H NMR ($CDCl_3$) δ 7.76 (d, J = 8.0 Hz, 2H), 7.47 (d, J = 8.0 Hz, 2H), 6.54 (s, 1H), 4.62 (dt, J^2_{HF} = 47.2 Hz, J^3_{HH} = 6.0 Hz, 2H), 3.97 (s, 2H), 3.50 (q, J = 7.2 Hz, 2H), 3.41 (q, J = 7.2 Hz, 2H), 2.76 (s, 3H), 2.59 (t, J = 7.2 Hz, 2H), 2.58 (s, 3H), 2.01 (dtt, 2H, J^3_{HF} = 25.6 Hz, J^3_{HH} = 7.2 & 6.0 Hz, 2H), 1.23 (t, J = 7.2 Hz, 3H), 1.12 (t, J = 7.2 Hz, 3H). ^{13}C NMR ($CDCl_3$) δ 169.7 [C], 157.6 [C], 154.5 [C], 147.4 [C], 145.2 [C], 133.0 [C], 131.6 [2xCH], 128.4 [2xCH], 123.5 [C], 108.4 [CH], 101.3 [C], 89.3 [C], 82.5 [d, J^1_{CF} = 164 Hz, CH_2], 81.2 [C], 42.2 [CH_2], 40.6 [CH_2], 29.5 [d, J^2_{CF} = 20 Hz, CH_2], 28.0 [CH_2], 24.3 [CH_3], 16.9 [CH_3], 15.4 [d, J^3_{CF} = 4 Hz, CH_2], 14.3 [CH_3], 13.0 [CH_3]. (ESI+)-MS: *m/z* 421 $[M+H]^+$. HR-(ESI+)-MS *m/z* calcd for $C_{25}H_{30}FN_4O$: 421.2404 $[M+H]^+$, found 421.2404.

***N*,*N*-Diethyl-2-(2-(4-(6-fluorohex-1-yn-1-yl)phenyl)-5,7-dimethylpyrazolo[1,5-a]pyrimidin-3-yl)acetamide (24).** Starting from 86 mg (0.199 mmol) of **20** and using the general procedure described above, compound **24** (33 mg, 0.076 mmol, 38 % yield) was isolated as a colorless oil. R_f (toluene/acetone 60/40, v/v): 0.52. t_R (HPLC A) = 1.33 min. ^{1}H NMR ($CDCl_3$) δ 7.76 (d, J = 8.0 Hz, 2H), 7.46 (d, J = 8.0 Hz, 2H), 6.54 (s, 1H), 4.52 (dt, J^2_{HF} = 47.2 Hz, J^3_{HH} = 6.0 Hz, 2H), 3.96 (s, 2H), 3.50 (q, J = 7.2 Hz, 2H), 3.42 (q, J = 7.2 Hz, 2H), 2.75 (s, 3H), 2.58 (s, 3H), 2.50 (t, J = 7.2 Hz, 2H), 1.89 (dtt, J^3_{HF} = 25.6 Hz, J^3_{HH} = 7.2 & 6.0 Hz, 2H), 1.75 (q^5, J = 7.2 Hz, 2H), 1.20 (t, J = 7.2 Hz, 3H), 1.10 (t, J = 7.2 Hz, 3H). ^{13}C NMR ($CDCl_3$) δ 169.6 [C], 157.6 [C], 154.9 [C], 147.5 [C], 146.0 [C], 132.7 [C], 131.6 [2xCH], 128.4 [2xCH], 123.8 [C], 108.3 [CH], 101.3 [C], 90.3 [C], 83.6 [d, J^1_{CF} = 164 Hz, CH_2], 81.1 [C], 42.2 [CH_2], 40.6 [CH_2], 29.5 [d, J^2_{CF} = 20 Hz, CH_2], 28.0 [CH_2], 24.4 [d, J^3_{CF}

= 5 Hz, CH_2], 23.9 [CH_3], 19.1 [CH_2], 16.9 [CH_3], 14.2 [CH_3], 13.0 [CH_3]. (ESI+)-MS: *m/z* 435 $[M+H]^+$. HR-(ESI+)-MS *m/z* calcd for $C_{26}H_{32}FN_4O$: 435.2560 $[M+H]^+$, found 435.2560.

General procedure for the synthesis of *N*,*N*-diethyl-2-(2-(4-(*n*-hydroxyalkyl)phenyl)-5,7-dimethylpyrazolo[1,5-a]pyrimidin-3-yl)acetamide (25-27). To a solution of the appropriate *N,N*-diethyl-2-(2-(4-(4-hydroxyalk-1-yn-1-yl)phenyl)-5,7-dimethylpyrazolo[1,5-*a*]pyrimidin-3-yl)acetamide (**18-20**) in dichloromethane (4-5 mL) was added 10 % palladium on charcoal (5 mol %). The reaction flask was degassed under vacuum and filled with hydrogen at 1 atm. and the reaction mixture was stirred at ambient temperature for 24 h. The mixture was then filtered on a silica pad and washed with a mixture of CH_2Cl_2/MeOH (8/2, v/v). The filtrate was concentrated to dryness and the residue was purified by silica gel column chromatography using CH_2Cl_2/MeOH (99/1 to 95/5 v/v) as eluent to afford the title compounds.

***N*,*N*-Diethyl-2-(2-(4-(4-hydroxybutyl)phenyl)-5,7-dimethylpyrazolo[1,5-a]pyrimidin-3-yl)acetamide (25).** Starting from 136 mg (0.302 mmol) of **18** and using the general procedure described above, compound **25** (94 mg, 0.230 mmol, 76 % yield) was isolated as a light yellow oil. R_f (CH_2Cl_2/MeOH 93/7, v/v): 0.26. ^{1}H NMR ($CDCl_3$) δ 7.71 (d, J = 8.0 Hz, 2H), 7.25 (d, J = 8.0 Hz, 2H), 6.50 (s, 1H), 3.91 (s, 2H), 3.63 (t, J = 6.4 Hz, 2H), 3.48 (q, J = 7.2 Hz, 2H), 3.40 (q, J = 7.2 Hz, 2H), 2.73 (s, 3H), 2.67 (t, J = 6.4 Hz, 2H), 2.62 (s, 3H), 1.72 (q^5, J = 6.4 Hz, 2H), 1.60 (q^5, J = 6.4 Hz, 2H), 1.19 (t, J = 7.2 Hz, 3H), 1.09 (t, J = 7.2 Hz, 3H). ^{13}C NMR ($CDCl_3$) δ 170.0 [C], 157.5 [C], 155.1 [C], 147.6 [C], 144.7 [C], 142.5 [C], 131.1 [C], 128.6 [2xCH], 128.5 [2xCH], 108.2 [CH], 100.9 [C], 62.6 [CH_2], 42.2 [CH_2], 40.5 [CH_2], 35.4 [CH_2], 32.2 [CH_2], 28.0 [CH_2], 27.4 [CH_2], 24.6 [CH_3], 16.9 [CH_3], 14.2 [CH_3], 13.0 [CH_3]. HR-(ESI+)-MS *m/z* calcd for $C_{24}H_{33}N_4O_2$: 409.2604 $[M+H]^+$, found 409.2620.

***N*,*N*-Diethyl-2-(2-(4-(4-hydroxypentyl)phenyl)-5,7-dimethylpyrazolo[1,5-a]pyrimidin-3-yl)acetamide (26).** Starting from 200 mg (0.478 mmol) of **19** and using the general procedure described above, compound **26** (80 mg, 0.189 mmol, 40 % yield) was isolated as a yellow oil. R_f (CH_2Cl_2/MeOH 9/1, v/v): 0.45. ^{1}H NMR ($CDCl_3$) δ 7.71 (d, J = 8.0 Hz, 2H), 7.26 (d, J = 8.0 Hz, 2H), 6.54 (s, 1H), 4.00 (s, 2H), 3.64 (t, J = 7.2 Hz, 2H), 3.50 (q, J = 7.2 Hz, 2H), 3.41 (q, J = 7.2 Hz, 2H), 2.77 (s, 3H), 2.67 (t, J = 8.0 Hz, 2H), 2.61 (s, 3H), 1.67 (q^5, J = 7.2 Hz, 2H), 1.60 (q^5, J = 7.2 Hz, 2H), 1.43 (m, 2H), 1.20 (t, J = 7.2 Hz, 3H), 1.10 (t, J = 7.2 Hz, 3H). ^{13}C NMR ($CDCl_3$) δ 169.9 [C], 157.4 [C], 154.8 [C], 147.8 [C], 145.0 [C], 142.7 [C], 131.0 [C], 128.6 [4xCH], 108.1 [CH], 101.0 [C], 62.9 [CH_2], 42.2 [CH_2], 40.5 [CH_2], 35.6 [CH_2], 32.6 [CH_2], 31.1 [CH_2], 28.1 [CH_2], 25.2 [CH_2], 24.5 [CH_3], 16.9 [CH_3], 14.2 [CH_3], 13.0 [CH_3]. HR-(ESI+)-MS *m/z* calcd for $C_{25}H_{35}N_4O_2$: 423.2760 $[M+H]^+$, found 423.2751.

***N*,*N*-Diethyl-2-(2-(4-(4-hydroxyhexyl)phenyl)-5,7-dimethylpyrazolo[1,5-a]pyrimidin-3-yl)acetamide (27).** Starting from 136 mg (0.314 mmol) of **20** and using the general procedure described above, compound **27** (99 mg, 0.226 mmol, 72 % yield) was isolated as a light yellow gum. R_f (CH_2Cl_2/MeOH 93/7, v/v): 0.30. ^{1}H NMR ($CDCl_3$) δ 7.71 (d, J = 8.0 Hz, 2H), 7.24 (d, J = 8.0 Hz, 2H), 6.51 (s, 1H), 3.92 (s, 2H), 3.61 (t, J = 6.8 Hz, 2H), 3.48 (q, J = 7.2 Hz, 2H), 3.40 (q, J = 7.2 Hz, 2H), 2.74 (s, 3H), 2.64 (t, J = 8.0 Hz, 2H), 2.54 (s, 3H), 1.64 (q^5, J = 6.8 Hz, 2H), 1.54 (q^5, J = 6.8 Hz, 2H), 1.34 (m, 4H), 1.18 (t, J = 7.2 Hz, 3H), 1.11 (t, J = 7.2 Hz, 3H). ^{13}C NMR ($CDCl_3$) δ 170.0 [C], 157.4 [C], 155.2 [C], 147.6 [C], 144.5 [C], 142.9 [C], 131.0 [C], 128.5 [4xCH], 108.2 [CH], 100.9 [C], 62.8 [CH_2], 42.2 [CH_2], 40.5 [CH_2], 35.6 [CH_2], 32.6 [CH_2], 31.3 [CH_2], 28.9 [CH_2], 28.0 [CH_2], 25.5 [CH_2], 24.5 [CH_3], 16.9 [CH_3], 14.2 [CH_3], 13.0 [CH_3]. HR-(ESI+)-MS *m/z* calcd for $C_{26}H_{37}N_4O_2$: 437.2917 $[M+H]^+$, found 437.2914.

General procedure for the synthesis of *N*,*N*-diethyl-2-(2-(4-(*n*-fluoroalkyl)phenyl)-5,7-dimethylpyrazolo[1,5-a]pyrimidin-3-yl)acetamide (28-30). To the appropriate *N,N*-diethyl-2-(2-(4-(*n*-hydroxyalkyl)phenyl)-5,7-dimethylpyrazolo[1,5-*a*]pyridimin-3-yl)acetamide (**25-27**) dissolved in toluene (2-4 mL) and dichloromethane (1.0-2.5 mL), were added 2-3 eq of a 50% Deoxo-Fluor® solution in toluene. The reaction mixture was stirred for 24 to 72 h at ambient temperature and additional Deoxo-Fluor® solution was added if required (TLC monitoring) to complete the conversion of the starting alcohol. The solvent was removed under vacuum and the resulting residue was dissolved in ethyl acetate (20 mL) and successively washed with water (20 mL) and brine (20 mL) before being dried over sodium sulfate, filtered and evaporated to dryness. The crude material was purified by silica gel column chromatography using CH_2Cl_2/MeOH (99/1 to 95/5, v/v) as eluent to yield the title compounds.

***N*,*N*-Diethyl-2-(2-(4-(4-fluorobutyl)phenyl)-5,7-dimethylpyrazolo[1,5-a]pyrimidin-3-yl)acetamide (28).** Starting from 140 mg (0.342 mmol) of **25** and using the general procedure described above, compound **28** (60 mg, 0.146 mmol, 43 % yield) was isolated as a yellow oil. R_f (CH_2Cl_2/MeOH 93/7, v/v): 0.59. t_R (HPLC A) = 1.25 min. ^{1}H NMR ($CDCl_3$) δ 7.73 (d, J = 8.0 Hz, 2H), 7.26 (d, J = 8.0 Hz, 2H), 6.52 (s, 1H), 4.46 (dt, J^2_{HF} = 47.2 Hz, J^3_{HH} = 5.6 Hz, 2H), 3.96 (s, 2H), 3.50 (q, J = 7.2 Hz, 2H), 3.41 (d, J = 7.2 Hz, 2H), 2.75 (s, 3H), 2.70 (t, J = 6.8 Hz, 2H), 2.57 (s, 3H), 1.80-1.70 (m, 4H), 1.23 (t, J = 7.2 Hz, 3H), 1.10 (t, J = 7.2 Hz, 3H). ^{13}C NMR ($CDCl_3$) δ 169.8 [C], 157.4 [C], 155.0 [C], 147.5 [C], 144.8 [C], 142.2 [C], 131.1 [C], 128.6 [2xCH], 128.5 [2xCH], 108.1 [CH], 101.0 [C], 83.9 [d, J^1_{CF} = 163 Hz, CH_2], 42.2 [CH_2], 40.6 [CH_2], 35.1 [CH_2], 29.8 [d, J^2_{CF} = 19 Hz, CH_2], 28.1 [CH_2], 26.8 [d, J^3_{CF} = 5 Hz, CH_2], 24.1 [CH_3],16.9 [CH_3], 14.2 [CH_3],13.0 [CH_3]. HR-ESI(+)-MS m/z calcd for $C_{24}H_{32}FN_4O$: 411.2560 $[M+H]^+$, found 411.2578.

***N*,*N*-Diethyl-2-(2-(4-(5-fluoropentyl)phenyl)-5,7-dimethylpyrazolo[1,5-a]pyrimidin-3-yl)acetamide (29).** Starting from 160 mg (0.378 mmol) of **26** and using the general procedure described above, compound **29** (88 mg, 0.208 mmol, 55 % yield) was isolated as colorless oil. R_f (heptane/acetone 50/50, v/v): 0.39. t_R (HPLC A) = 1.35 min. ^{1}H NMR ($CDCl_3$) δ 7.72 (d, J = 8.0 Hz, 2H), 7.25 (d, J = 8.0 Hz, 2H), 6.51 (s, 1H), 4.43 (dt, J^2_{HF} = 47.6 Hz, J^3_{HH} = 6.0 Hz, 2H), 3.95 (s, 2H), 3.49 (q, J = 7.2 Hz, 2H), 3.41 (q, J = 7.2 Hz, 2H), 2.74 (s, 3H), 2.67 (t, J = 7.6 Hz, 2H), 2.56 (s, 3H), 1.80-1.65 (m, 4H), 1.46 (m, 2H), 1.20 (t, J = 7.2 Hz, 3H), 1.10 (t, J = 7.2 Hz, 3H). ^{13}C NMR ($CDCl_3$) δ 169.8 [C], 157.4 [C], 155.0 [C], 147.8 [C], 145.1 [C], 142.6 [C], 131.0 [C], 128.6 [2xCH], 128.5 [2xCH], 108.1 [CH], 101.0 [C], 84.0 [d, J^1_{CF} = 163 Hz, CH_2], 42.2 [CH_2], 40.5 [CH_2], 35.5 [CH_2], 30.9 [CH_2], 30.2 [d, J^2_{CF} = 19 Hz, CH_2], 28.1 [CH_2], 24.7 [d, J^3_{CF} = 6 Hz, CH_2], 24.2 [CH_3], 16.9 [CH_3], 14.2 [CH_3], 13.0 [CH_3]. HR-ESI(+)-MS m/z calcd for $C_{25}H_{34}FN_4O$: 425.2717 $[M+H]^+$, found 425.2718.

***N*,*N*-Diethyl-2-(2-(4-(6-fluorohexyl)phenyl)-5,7-dimethylpyrazolo[1,5-a]pyrimidin-3-yl)acetamide (30).** Starting from 140 mg (0.320 mmol) of **27** and using the general procedure described above, compound **30** (82 mg, 0.186 mmol, 58 % yield) was isolated as an orange oil. R_f (CH_2Cl_2/MeOH 93/7, v/v): 0.63. t_R (HPLC A) = 1.43 min. ^{1}H NMR ($CDCl_3$) δ 7.72 (d, J = 8.0 Hz, 2H), 7.25 (d, J = 8.0 Hz, 2H), 6.51 (s, 1H), 4.43 (dt, J^2_{HF} = 47.6 Hz, J^3_{HH} = 6.0 Hz, 2H), 3.94 (s, 2H), 3.49 (q, J = 7.2 Hz, 2H), 3.41 (q, J = 7.2 Hz, 2H), 2.74 (s, 3H), 2.65 (t, J = 7.6 Hz, 2H), 2.55 (s, 3H), 1.75-1.62 (m, 4H), 1.45-1.30 (m, 4H), 1.20 (t, J = 7.2 Hz, 3H), 1.10 (t, J = 7.2 Hz, 3H). ^{13}C NMR ($CDCl_3$) δ 169.9 [C], 157.4 [C], 155.5 [C], 147.3 [C], 145.0 [C], 142.8 [C], 130.9 [C], 128.5 [4xCH], 108.1 [CH], 101.0 [C], 84.1 [d, J^1_{CF} = 163 Hz, CH_2], 42.2 [CH_2], 40.5 [CH_2], 35.6 [CH_2], 31.2 [CH_2], 30.3 [d, J^2_{CF} = 19 Hz, CH_2], 28.7 [CH_2], 28.1 [CH_2], 25.0 [d, J^3_{CF} = 5 Hz, CH_2], 24.2 [CH_3], 16.9

[CH_3], 14.2 [CH_3], 13.0 [CH_3]. HR-ESI(+)-MS m/z calcd for $C_{26}H_{36}FN_4O$: 439.2873 $[M+H]^+$, found 439.2889.

3-(4-(3-(2-(Diethylamino)-2-oxoethyl)-5,7-dimethylpyrazolo[1,5-a]pyrimidin-2-yl)phenyl)propyl 4-methylbenzenesulfonate (31). To 150 mg of *N*,*N*-diethyl-2-(2-(4-(3-hydroxypropyl)phenyl)-5,7-dimethylpyrazolo[1,5-a]pyrimidin-3-yl)acetamide **11** (0.381 mmol) dissolved in dichloromethane (5 mL), were added *p*-toluenesulfonyl chloride (87 mg, 0.457 mmol) and triethylamine (106 μL, 0.761 mmol). The reaction mixture was stirred at ambient temperature for 16 h and quenched with addition of a 1.0 M aqueous hydrochloric acid solution solution (30 mL). The product was extracted with ethyl acetate (20 mL) and the resulting organic layer washed with brine before being dried over sodium sulfate, filtered and evaporated to dryness. The resulting residue was purified by silica gel column chromatography using CH_2Cl_2/MeOH (98/2, v/v) as eluent to yield compound **31** (178 mg, 0.325 mmol, 85 % yield) as a light yellow oil. R_f (CH_2Cl_2/MeOH 92/8, v/v): 0.35. ^{1}H NMR (CD_2Cl_2) δ 7.78 (d, J = 8.0 Hz, 2H), 7.67 (d, J = 8.0 Hz, 2H), 7.38 (d, J = 8.0 Hz, 2H), 7.17 (d, J = 8.0 Hz, 2H), 6.56 (s, 1H), 4.03 (t, J = 6.4 Hz, 2H), 3.88 (s, 2H), 3.49 (q, J = 7.2 Hz, 2H), 3.37 (q, J = 7.2 Hz, 2H), 2.73 (s, 3H), 2.69 (t, J = 7.6 Hz, 2H), 2.53 (s, 3H), 2.45 (s, 3H), 1.98 (m, 2H), 1.22 (t, J = 7.2 Hz, 3H), 1.09 (t, J = 7.2 Hz, 3H). ^{13}C NMR (CD_2Cl_2) δ 169.6 [C], 157.6 [C], 154.3 [C], 147.6 [C], 145.0 [C], 144.8 [C], 140.7 [C], 133.0 [C], 131.8 [C], 129.8 [2×CH], 128.5 [2×CH], 128.4 [2×CH], 127.7 [2×CH], 108.2 [CH], 101.0 [C], 69.7 [CH_2], 42.1 [CH_2], 40.4 [CH_2], 31.1 [CH_2], 30.3 [CH_2], 27.9 [CH_2], 24.3 [CH_3], 21.3 [CH_3], 16.5 [CH_3], 14.0 [CH_3], 12.8 [CH_3]. ESI(+)-MS (m/z): 549 $[M+H]^+$, 571 $[M+Na]^+$, 587 $[M+K]^+$. HR-ESI(+)-MS m/z calcd for $C_{30}H_{37}N_4O_4S$: 549.2536 $[M+H]^+$, found 549.2541.

5-(4-(3-(2-(Diethylamino)-2-oxoethyl)-5,7-dimethylpyrazolo[1,5-a]pyrimidin-2-yl)phenyl)pent-4-yn-1-yl 4-methylbenzenesulfonate (32). To 200 mg of *N*,*N*-diethyl-2-(2-(4-(5-

hydroxypent-1-yn-1-yl)phenyl)-5,7-dimethylpyrazolo[1,5-a]pyrimidin-3-yl)acetamide **19** (0.478 mmol) dissolved in dichloromethane (8 mL), were added at 0°C, *p*-toluenesulfonic anhydride (170 mg, 0.520 mmol) and triethylamine (166 µL, 1.20 mmol). The reaction mixture was stirred at ambient temperature for 5 h and quenched with addition of a 1.0 M aqueous hydrochloric acid solution solution (50 mL). The product was extracted with ethyl acetate (50 mL) and the resulting organic layer washed with brine before being dried over sodium sulfate, filtered and evaporated to dryness. The resulting residue was purified by silica gel column chromatography using CH_2Cl_2/MeOH (98/2, v/v) as eluent to yield compound **32** (150 mg, 0.263 mmol, 55 % yield) as a white solid. R_f (CH_2Cl_2/MeOH 95/5, v/v): 0.45. ^{1}H NMR ($CDCl_3$) δ 7.80 (d, J = 8.0 Hz, 2H), 7.76 (d, J = 8.0 Hz, 2H), 7.36 (d, J = 8.0 Hz, 2H), 7.31 (d, J = 8.0 Hz, 2H), 6.53 (s, 1H), 4.21 (t, J = 5.6 Hz, 2H), 3.94 (s, 2H), 3.51 (q, J = 7.2 Hz, 2H), 3.40 (q, J = 7.2 Hz, 2H), 2.74 (s, 3H), 2.55 (s, 3H), 2.49 (t, J = 6.8 Hz, 2H), 2.39 (s, 3H), 1.94 (m, 2H), 1.23 (t, J = 7.2 Hz, 3H), 1.11 (t, J = 7.2 Hz, 3H). ^{13}C NMR ($CDCl_3$) δ 169.7 [C], 157.6 [C], 154.4 [C], 147.0 [C], 145.0 [C], 144.8 [C], 133.1 [C], 132.8 [C], 131.6 [2×CH], 129.8 [2×CH], 128.4 [2×CH], 127.8 [2×CH], 123.3 [C], 108.4 [CH], 101.3 [C], 88.4 [C], 81.7 [C], 68.9 [CH_2], 42.2 [CH_2], 40.6 [CH_2], 28.0 [CH_2], 27.9 [CH_2], 24.3 [CH_3], 21.6 [CH_3], 16.8 [CH_3], 15.7 [CH_2], 14.3 [CH_3], 13.0 [CH_3]. ESI(+)-MS (m/z): 573 $[M+H]^+$. HR-ESI(+)-MS m/z calcd for $C_{32}H_{37}N_4O_4S$: 573.2536 $[M+H]^+$, found 573.2524.

Radiochemistry. Radioisotope production. No-carrier-added fluorine-18 (half-life: 109.8 min) was produced via the [^{18}O(p,n)^{18}F] nuclear reaction by irradiation of a 2 mL [^{18}O]water (> 97 % enriched, Rotem, CortecNet, Paris, France) target on an IBA Cyclone-18/9 (IBA, Belgium) cyclotron (18 MeV proton beam) and the aqueous radioactive solution was then transferred to the appropriate hot cell. Target hardware: Commercial, 2 mL, two-port, stainless steel target holder equipped with a domed-end niobium cylinder insert. **Target to hot cell liquid-transfer system**. 50 m PTFE line (0.8

mm internal diameter ; 1/16 inch external diameter), 2.0 bar helium drive pressure, transfer time 2-3 min. Typical production of [^{18}F]fluoride at the end of bombardment for a 30-61 min (14.0 – 25.7 μA.h) irradiation: 26.6 – 48.0 GBq (720–1.30 mCi). **Radiosynthesis.** Radiofluorination were performed on a slightly modified TRACERLab FX-FN synthesiser[53] (GE Medical Systems, Germany) and the data were collected and processed by the TRACERLab FX software (GE Healthcare). HPLC purification at the semi-preparative scale was performed with the following equipment and conditions: System equipped with a Waters 515 pump, a UV detector K-2501 (Knauer, Germany) and a radioactivity gamma detector (integrated in the synthesiser); column: semi-preparative X-Terra^{TM} RP18, 300×7.8 mm, 7 μm (Waters); eluent 0.1 M aqueous NH_4OAc (pH 10)/CH_3CN: 60/40 (v:v); flow rate: 6 mL/min; temperature: rt; absorbance detection at λ = 254 nm. The radiotracer is finally automatically formulated in a saline/ethanol 80:20 (v:v) solution. **Quality control.** The radiotracer preparations were visually inspected for clarity, absence of colour and particulates. An aliquot of the preparation was removed for determination of pH using standard pH-paper (Duotest®, Macherey-Nagel, pH 1-12, Hoerdt, France). Chemical and radiochemical purities were also assessed on this aliquot by HPLC (analytical HPLC), with an authentic sample of tracer (**1** or **23)**. The following equipment and conditions were used: Equipment: Waters (Guyancourt, France) Alliance 2965 equipped with a UV spectrophotometer (Photodiode Array Detector, Waters 2996) and a Berthold LB509 radioactivity detector; column: analytical Symmetry® C18, 50×4.6 mm, 3.5 μm (Waters); conditions: isocratic elution with solvA/solvB: 35/65 (v:v) (solvent A: H_2O containing Low-UV PIC® B7 reagent (20 mL for 1 L); solvent B: H_2O/CH_3CN: 30:70 (v:v) containing Low-UV PIC® B7 reagent (20 mL for 1 L)); flow rate: 2.0 mL/min; temperature: rt; absorbance detection at λ = 254 nm. Particular attention was paid to the absence of non-radioactive precursor for labelling (**31** or **32**). Chemical and radiochemical stabilities of the entire preparation were tested by HPLC

(analytical HPLC) at regular 15 min intervals during 150 min. Specific radioactivity of the radiotracer was calculated from three consecutive HPLC (analytical HPLC) analyses (average) and determined as follows: the area of the UV absorbance peak corresponding to the radiolabelled product was measured (integrated) on the HPLC-chromatogram and compared with a standard curve relating mass to UV absorbance.

***N*,*N*-diethyl-2-(2-(4-(3-[^{18}F]fluoropropyl)phenyl)-5,7-dimethylpyrazolo[1,5-a]pyrimidin-3-yl)acetamide ([^{18}F]12).** The cyclotron produced irradiated water, once transferred to the module, was aspirated through a Sep-Pak® Light Accell™ Plus QMA-cartridge (Waters) to fix [^{18}F]fluoride anions and remove the [^{18}O]enriched water. [^{18}F]Fluoride (33-52 GBq) was then eluted with a solution of K_{222} (12-15 mg) and K_2CO_3 (1.5 mg) in water/acetonitrile (30/70 v/v, 1 mL) into the reaction vessel. The dried, no-carrier-added, K[^{18}F]F-K_{222} complex was prepared by evaporation of the solution with heating under vacuum (60 °C for 7 min followed by 120 °C for 5 min). [^{18}F]**12** was obtained by addition of a solution of the precursor for labelling **31** (4.0 to 4.5 mg) in the appropriate solvent (CH_3CN or DMSO, 700 µL) to the dried K[^{18}F]F-K_{222} complex and fluorine-18 incorporation was evaluated in CH_3CN by heating the reaction mixture at 100 °C either for 5 min or 10 min, or in DMSO by heating the reaction mixture for 5 min at 165 °C. After this period of heating, the reaction mixture was cooled to 50°C and diluted with HPLC solvent (2 mL) before being transferred under pressure trough a Sep-Pak® Alumina N cartridge (Waters) and finally collected in a HPLC tube. The reaction vessel was rinsed with HPLC solvent (2 mL) and the resulting solution transferred to the HPLC tube *via* the Sep-Pak® Alumina N cartridge. The crude solution (4.7 mL) collected in the HPLC tube was injected onto reverse phase HPLC column (semi-preparative HPLC) and the product fraction of [^{18}F]**12** was collected, diluted with water (10 mL), passed through a Sep-Pak®Plus C18 cartridge (Waters) to fix the radiotracer and remove residual acetonitrile or salts by washing the

cartridge with additional water (5 mL) before elution of the cartridge with ethanol (2 mL) and dilution of the ethanolic solution of [^{18}F]**12** with 0.9% aq. NaCl solution (8 mL) for *i.v.* injection.

N,N-diethyl-2-(2-(4-(5-[^{18}F]fluoropent-1-yn-1-yl)phenyl)-5,7-dimethylpyrazolo[1,5-a]pyrimidin-3-yl)acetamide ([^{18}F]23). The preparation of [^{18}F]**23** was achieved using the same procedure as described above for the preparation of [^{18}F]**12**, starting from the precursor for labelling **32**, and using a heating period of 10 min at 100 °C in CH_3CN.

In vitro competition assays (Table 1). Binding affinities for the TSPO (Ki) were determined using membrane homogenates from rat heart and screened against [^{3}H]PK11195 (K_d = 1.8 nM, C = 0.2 nM). Affinities for the CBR were determined at a unique concentration (1 μM), using membrane homogenates from rat cerebral cortex and screened against [^{3}H]flunitrazepam (K_d = 2.1 nM, C = 0.4 nM).

Partition coefficient (log $D_{7.4}$) and LipE calculation (Table 1). $LogD_{7.4}$ (*n*-octanol/buffer pH 7.4 partition coefficient) values were determined based on a validated and standardized HPLC method, by conversion of the recorded retention time for each compound (correlation between retention times and known logD values of similar compounds). HPLC conditions: Alliance 2695 - PDA Waters, X-Terra MS C18 (4.6 x 20 mm, 3.5 μm) column ; mobile phase 5 mM MOPS / $(CH_3)_4NOH$ pH 7.4 (A), 5 % MOPS / $(CH_3)_4NOH$ (100 mM, pH 7.4) / 95 % CH_3CN (B) ; gradient (A / B): 98:2 (0.5 min), 0:100 (4.8 min), 98:2 (1.6 min) ; 1.2 mL/min ; 25 °C ; detection at 254 nm. LipE was calculated as follows: $LipE = pIC_{50} - logD_{7.4}$.

***In vitro* metabolism (Table 2).** Compounds were incubated with hepatic microsomal fractions (male CD1 mouse, male Sprague-Dawley rat or humans (BD pool)) using the following experimental

conditions throughout the study: microsomal proteins concentration = 1 mg/mL; bovine serum albumin (BSA) concentration = 1 mg/mL; substrate concentration = 5 µM; cofactor (if used, see below): 1 mM aq. NADPH. For each compound to be tested, 2 samples were prepared: Sample A: microsomal incubation, 0 min, without cofactor; Sample B: microsomal incubation, 20 min, with cofactor. Enzyme activity was stopped with 1 volume of ACN, and proteins removed by centrifugation. The supernatant fluids were then analysed by HPLC/ESI-MS/MS with the mass spectrometer set in selected ion recording (SIR) in positive mode. The data were collected and processed using MassLynx 4.0 software from Waters-Micromass, leading to quantification of the unchanged tested compound. Analytical HPLC conditions: C18 (125 x 2.1 mm, 3 µm) column; mobile phase: (A) H_2O containing NH_4OAc (0.25 g/L) and HCO_2H (2 mL/L), (B) ACN / MeOH (80 / 20) containing NH_4OAc (0.15 g/L), HCO_2H (2 mL/L) and H_2O (10 mL/L) ; gradient (A/B): 90:10 (0.75 min), 0:100 (3.25 min), 90:10 (2.0 min) ; 0.3 mL/min; injection volume: 10 µL. The percentages of biotransformation, consisting in oxidative reactions as well as non-co-factor-dependent reactions such as ester bond hydrolysis, were calculated using the following formula and are reported in Table 2:

$$[\%\ \text{biotransformation}] = [1 - (\frac{\text{Peak Area corresponding to unchanged compound in Sample B}}{\text{Peak Area corresponding to unchanged compound in Sample A}})] \times 100$$

***In vitro* autoradiographies and *in vivo* small animal PET studies. Acute neuroinflammatory animal model.** Striatal AMPA-mediated excitotoxicity and acute local neuroinflammation in the brain of Wistar rats was induced according to reported procedures.[23,34,52] The protocol used includes a stereotactic injection in the right striatum of 0.5 µL of AMPA ((*R,S*)-*α*-amino-3-hydroxy-5-methyl-4-isoxazolopropionic acid, 15 mM in phosphate buffered saline (PBS) buffer) in anaesthetised and normothermically-controlled animals followed by a resting period of 7 days. ***In vitro* brain**

autoradiographies. Brain slices of unilaterally AMPA-lesioned animals were prepared according to reported procedures.[23,34,52] The protocol used includes decapitation of the animals under terminal anaesthesia, quick brain removal and freezing in cold (-80°C, dry-ice) isopentane followed by coronally, 10 µm-thick slicing of the brain at the level of the lesion. Then, adjacent brain slices (36 slices from the center of the lesioned area) were taken and incubated for 20 min in Tris Buffer (TRIZMA pre-set Crystals, Sigma®, adjusted at pH 7.4 at 4°C, 50 mM with NaCl 120 mM) containing the radiotracer alone [^{18}F]**12** or [^{18}F]-**23**, 90-111 MBq, 500-600 MBq/L, 5-10 nM), or the radiotracer and PK11195 (20 µM), the radiotraceur and its non-labelled version (20 µM) as well as the radiotracer and flumazenil (20 µM). Brain sections were then washed 2 times for 2 min and once for 10 sec with cold (4°C) buffer, then exposed on a Phosphor-Imager screen overnight. Autoradiograms were scanned and then analysed using the ImageJ software (developed by the National Institutes of Health). A region of interest (ROI) was manually drawn around the core of the lesion, and an identical area was copy-pasted symmetrically into the contralateral hemisphere. Binding in the ROI was then expressed as the number of counts per surface unit. The target-to-background ratio (TBR) was calculated as the ratio of the binding in the lesioned versus the contralateral hemisphere. **Small animal PET studies.** Rats (n = 4, 355 ± 22.5 g) were imaged with the radiotracer ([^{18}F]**12** or [^{18}F]**23**) seven days after intrastriatal injection of AMPA (see above) using a commercially available, small-animal-dedicated, INVEON PET/CT or PET only tomograph (Siemens, Munich, Germany). Anaesthesia of animals was induced by a mixture of isoflurane and O_2 (3% / 97%). Animals were then placed in a home-made stereotaxic frame compatible with PET acquisition, maintained anaesthetised by using only a 1.5%-2.5% mixture of isoflurane in O_2 and maintained normothermic using a heating pad (Heater Pad Biovet®, m2m Imaging Corp., Cleveland, OH, USA). Animals were injected with the radiotracer (0.9-1.1 mCi, 3 to 20 nmoles, 350 to 500 µL))

in the caudal lateral vein using a 24 gauge catheter. Imaging started at the time of injection of the radiotracer and lasted for 60 min. 3D-PET acquisitions were performed with the coincidence time window set to 3.432 nsec and the energy levels of discrimination set to 350 keV and 650 keV. The list mode file of the emission scans was histogrammed into 24 dynamic frames (3 x 30 sec, 5 x 60 sec, 5 x 2 min, 3 x 3 min, 3x 3 min, 4 x 5 min and 1 x 10 min) with a maximum ring difference of 79 and a span of 3. A 3D attenuation correction file was generated with correction factors either measured using an external cobalt-57 point source (PET only tomograph) or using the CT X-ray source (PET/CT tomograph). The emission sinograms (i.e., each frame) were then normalized and corrected for attenuation and radioactivity decay. 3D images were finally reconstructed with the Fourier rebinning (FORE) and ordered-subsets expectation-maximization, 2-dimensional (OSEM 2D) algorithms (16 subsets and 4 iterations). Image analysis and quantification of radioactivity uptake in volumes of interest (VOIs) were performed using Brain-Visa / Anatomist version 3.1 (developed in-house[54]). On the ipsilateral side, delineation of the lesion area was made by manual segmentation on the summed-frame images spanning the last 30 min of the PET acquisition. A region of interest (ROI) was drawn on each adjacent transaxial section containing the lesion and combined to define a volume of interest (VOI). On the contralateral side, an ovoid VOI (4 x 4 x 4 voxels, 22 mm^3) was manually positioned in the center of the striatum. These VOIs were then projected onto all dynamic frames and the resulting time activity curves were then normalized for the percentage of injected dose per milliliter (%ID/mL).

ASSOCIATED CONTENT

Supporting information availability:

^{1}H and ^{13}C NMR spectra as well as HRMS data of synthesised and tested compounds **12, 21–24** and **28–32**.

AUTHOR INFORMATION

Corresponding Author

*Phone: +33 (0)1 69 08 13 18. E-mail: annelaure.damont@cea.fr

Notes

The authors declare no competing financial interest.

ACKNOWLEDGMENTS

This work was supported by CEA-I^{2}BM intramural programs, as well as the European Union's Seventh Framework Programme [FP7/2007-2013] INMiND (Grant agreement n° HEALTH-F2-2011-278850). The authors would like to thank former students Helene Gaudy and Alex Ching; radiochemists Fabien Caillé, Stéphane Demphel and Stéphane Le Helleix; cyclotron operators Daniel Gouel, Christophe Lechêne and Tony Catarina for their participation in this work. The authors also wish to thank LGCR Analytical Sciences (Sanofi, Chilly Mazarin) for log$D_{7.4}$ measurements and DMPK (Sanofi, Montpellier) for preliminary metabolism studies. HRMS determination has benefited from the facilities and expertise of the Small Molecule Mass Spectrometry platform of IMAGIF, Gif-sur-Yvette, France (www.imagif.cnrs.fr).

ABBREVIATIONS USED

CBR, central benzodiazepine receptor; d.c., decay-corrected; DPA, 3,5-dimethylpyrazolo[1,5-a]pyrimidin-3-yl acetamide; EOB, end of bombardment; EOS, end of synthesis; LipE, lipophilic

efficiency; PTFE, polytetrafluoroethylene; RCY, radiochemical yield; ROI, region of interest; SRA, specific radioactivity; TBR, target-to-background ratio; TSPO, translocator protein 18 kDa (formerly known as peripheral benzodiazepine receptor, PBR); VOI, volume of interest.

REFERENCES

(1) Dollé, F.; Luus, C.; Reynolds, A.; Kassiou, M. Radiolabelled molecules for imaging the translocator protein (18 kDa) using positron emission tomography. *Curr. Med. Chem.* **2009**, *16*, 2899–2923.

(2) Shah, F.; Pike, V. W.; Turton, D. R. Syntheses of homochiral ^{11}C-labelled radioligands for peripheral benzodiazepine binding sites. *J. Labelled Compd. Radiopharm.* **1993**, *32*, S166-168.

(3) Thominiaux, C.; Demphel, S.; Damont, A.; Boutin, H.; Rooney, T.; Tavitian, B.; Dollé, F. Carbon-11-labelling of three PK11195 analogues: [^{11}C]PK13015, [^{11}C]PK12090 and [^{11}C]PK14045. *J. Labelled Compd. Radiopharm.* **2013**, *56*, S291.

(4) Castellano, S.; Taliani, S.; Milite, C.; Pugliesi, I.; Da Pozzo, E.; Rizzetto, E.; Bendinelli, S.; Costa, B.; Cosconati, S.; Greco, G.; Novellino, E.; Sbardella, G.; Stefancich, G.; Martini, C.; Da Settimo, F. Synthesis and biological evaluation of 4-Phenylquinazoline-2-carboxamides designed as a novel class of potent ligands of the translocator protein. *J. Med. Chem.* **2012,** *55,* 4506–4510.

(5) Castellano, S.; Taliani, S.; Viviano, M.; Milite, C.; Da Pozzo, E.; Costa, B.; Barresi, E.; Bruno, A.; Cosconati, S.; Marinelli, L.; Greco, G.; Novellino, E.; Sbardella, G.; Da Settimo, F.; Martini, C. Structure–activity relationship refinement and further assessment of 4-Phenylquinazoline-2-carboxamide translocator protein ligands as antiproliferative agents in human glioblastoma tumors. *J. Med. Chem.* **2014,** *57*, 2413–2428.

(6) Brouwer, C.; Jenko, K.; Zoghbi, S. S.; Innis, R. B.; Pike, V. W. Development of N-Methyl-(2-arylquinolin-4-yl)oxypropanamides as leads to PET radioligands for translocator protein (18 kDa). *J. Med. Chem.* **2014,** *57,* 6240−6251.

(7) Marangos, P. J.; Patel, J.; Boulenger J. P.; Clark-Rosenberg, R. Characterization of peripheral-type benzodiazepine binding sites in brain using [^{3}H]Ro 5-4864. *Mol. Pharmacol.* **1982**, *22*, 26−32.

(8) Schoemaker, H.; Boles, R. G.; Horst, W. D.; Yamamura, H. I. Specific high-affinity binding sites for [^{3}H]Ro 5-4864 in rat brain and kidney. *J. Pharmacol. Exp. Ther.* **1983**, *225*, 61−69.

(9) Turton, D. R.; Pike, V. W.; Cartoon, M.; Widdowson, D. A. Preparation of a potential marker for glial cells – (*N*-methyl-^{11}C) Ro5-4864. *J. Labelled Compd. Radiopharm.* **1984**, *21*, 1209−1210.

(10) Zhang, M. R.; Kida, T.; Noguchi, J.; Furutsuka, K.; Maeda, J.; Suhara, T.; Suzuki, K. [^{11}C]DAA1106: radiosynthesis and *in vivo* binding to peripheral benzodiazepine receptors in mouse brain. *Nucl. Med. Biol.* **2003**, *30*, 513−519.

(11) Probst, K. C., Izquierdo, D.; Bird, J. L.: Brichard, L.; Franck, D.; Davies, J. R.; Fryer, T. D.; Richards, H. K.; Clark, J. C.; Davenport, A. P.; Weissberg, P. L.; Warburton, E. A. Strategy for improved [^{11}C]DAA1106 radiosynthesis and *in vivo* peripheral benzodiazepine receptor imaging using microPET, evaluation of [^{11}C]DAA1106. *Nucl. Med. Biol*. **2007**, *34*, 439−446.

(12) Takano, A.; Arakawa, R.; Ito, H.; Tateno, A.; Takahashi, H.; Matsumoto, R.; Okubo, Y.; Suhara, T. Peripheral benzodiazepine receptors in patients with chronic schizophrenia: a PET study with [^{11}C]DAA1106. *Int. J. Neuropsychopharmacol.* **2010**, *13*, 943−950.

(13) Zhang, M. R.; Maeda, J.; Furutsuka, K.; Yoshida, Y.; Ogawa, M.; Suhara, T.; Suzuki, K. [^{18}F]FMDAA1106 and [^{18}F]FEDAA1106: two positron-emitter labeled ligands for peripheral benzodiazepine receptor (PBR). *Bioorg. Med. Chem. Lett.* **2003**, *13*, 201−204.

(14) Briard, E.; Shah, J.; Musachio, J. L.; Zoghbi, S. S.; Fujita, M.; Imaizumi, M.; Cropley, V.; Innis, R. B.; Pike, V. W. Synthesis and evaluation of a new ^{18}F-labeled ligand for PET imaging of brain peripheral benzodiazepine receptors. *J. Labelled Compd. Radiopharm.* **2005**, *48*, S4.

(15) Wang, M.; Gao, M.; Miller, K. D.; Zheng, Q. H. Synthesis of [^{11}C]PBR06 and [^{18}F]PBR06 as agents for positron emission tomographic (PET) imaging of the translocator protein (TSPO). *Steroids* **2011**, *76*, 1331−1340.

(16) Zhang, M. R.; Kumata, K.; Suzuki, K. A practical route for synthesizing a PET ligand containing [^{18}F]fluorobenzene using reaction of diphenyliodonium salt with [^{18}F]F^{-}. *Tetrahedron Lett.* **2007**, *48*, 8632−8635.

(17) Briard, E.; Hong, J.; Musachio, J. L.; Zoghbi, S. S.; Fujita, M.; Imaizumi, M.; Cropley, V.; Innis, R. B., Pike, V. W. Synthesis and evaluation of two candidate ^{11}C-labeled radioligands for brain peripheral benzodiazepine receptors. *J. Labelled Compd. Radiopharm.* **2005**, *48*, S71.

(18) Briard, E.; Zoghbi, S. S.; Imaizumi, M.; Gourley, J. P.; Hong, J.; Cropley, V.; Fujita, M.; Innis, R. B.; Pike, V. W. Synthesis and evaluation in monkey of two sensitive ^{11}C-labeled aryloxyanilide ligands for imaging brain peripheral benzodiazepine receptors in vivo. *J. Med. Chem*. **2008**, *51*, 17**–**30.

(19) Wilson, A. A.; Garcia, A.; Parkes, J.; McCormick, P.; Stephenson, K. A.; Houle, S.; Vasdev, N. Radiosynthesis and initial evaluation of [^{18}F]-FEPPA for PET imaging of peripheral benzodiazepine receptors. *Nucl. Med. Biol.* **2008**, *35*, 305−314.

(20) Damont, A.; Boisgard, R.; Kuhnast, B.; Lemée, F.; Raggiri, G.; Scarf, A. M.; Da Pozzo, E.; Selleri, S.; Martini, C.; Tavitian, B.; Kassiou, M.; Dollé, F. Synthesis of 6-[^{18}F]fluoro-PBR28, a novel radiotracer for imaging the TSPO 18 kDa with PET. *Bioorg. Med. Chem. Lett*. **2011**, *21*, 4819**–**4822.

(21) Taliani, S.; Pugliesi, I.; Da Settimo, F. Structural requirements to obtain highly potent and selective 18 kDa Translocator Protein (TSPO) Ligands. *Curr. Top. Med. Chem.* **2011**, *11*, 860–886.

(22) Thominiaux, C.; Mattner, F.; Greguric, I.; Boutin, H.; Chauveau, F.; Kuhnast, B.; Grégoire, M.-C.; Loc′h, C.; Valette, H.; Bottlaender, M.; Hantraye, P.; Tavitian, B.; Katsifis, A.; Dollé, F. Radiosynthesis of 2-[6-chloro-2-(4-iodophenyl)imidazo[1,2-*a*]pyridin-3-yl]-*N*-ethyl-*N*-[^{11}C]methyl-acetamide, [^{11}C]CLINME, a novel radioligand for imaging the peripheral benzodiazepine receptors with PET. *J. Labelled Compd. Radiopharm.* **2007**, *50*, 229–236.

(23) Boutin, H.; Chauveau, F.; Thominiaux, C.; Kuhnast, B.; Grégoire, M. C.; Jan, S.; Trebossen, R.; Dollé, F.; Tavitian, B.; Mattner, F.; Katsifis, A. *In vivo* imaging of brain lesions with [^{11}C]CLINME, a new PET radioligand of peripheral benzodiazepine receptors. *Glia* **2007**, *55*, 1459–1468.

(24) Bourdier, T.; Henderson, D.; Fookes, C. J.; Lam, P.; Mattner, F.; Fulham, M.; Katsifis, A. Synthesis of [^{11}C]PBR170, a novel imidazopyridine, for imaging the translocator protein with PET. *Appl. Radiat. Isot.* **2014**, *90*, 46–52.

(25) Bourdier, T.; Mattner, F.; Fookes, C.; Pham, T.; Loc'h, C.; Katsifis, A. *In vivo* evaluation of a [^{18}F]-labelled imidazopyridine (PBR170), for the study of the translocator protein using PET. *J. Labelled Compd. Radiopharm.* **2011**, *54*, S274.

(26) Bourdier, T.; Henderson, D.; Lam, P.; Fookes, C.; Mattner, F.; Greguric, I.; Pham, T.; Eberl, S.; Wen, L.; Katsifis, A. Labelling and *in vivo* evaluation in baboons of a novel [^{11}C]-carbon labelled imidazopyridine, for the study of the peripheral benzodiazepine receptors using PET. *J. Labelled Compd. Radiopharm.* **2009**, *52*, S347.

(27) Sekimata, K.; Hatano, K.; Ogawa, M.; Abe, J.; Magata, Y.; Biggio, G.; Serra, M.; Laquintana, V.; Denora, N.; Latrofa, A.; Trapani, G.; Liso, G.; Ito, K. Radiosynthesis and *in vivo* evaluation of *N*-

[^{11}C]methylated imidazopyridineacetamides as PET tracers for peripheral benzodiazepine receptors. *Nucl. Med. Biol.* **2008**, *35*, 327–334.

(28) Pham, T.; Mattner, F.; Fookes, I.; Greguric, I.; berghofer, P.; Ballantyne, P.; Liu, X.; Shepherd, R.; Jackson, T.; Katsifis, A. Synthesis and evaluation of (^{18}F) labelled imidazopyridines, for the study of peripheral benzodiazepine binding sites using PET. *J. Labelled Compd. Radiopharm.* **2007**, *50*, S377.

(29) Fookes, C.; Pham, T.; Mattner, F.; Greguric, I.; Loc'h, C.; Liu, X.; Berghofer, P.; Shepherd, R.; Grégoire, M.-C.; Katsifis, A. Synthesis and biological evaluation of substituted [^{18}F]imidazo[1,2-a]pyridines and [^{18}F]pyrazolo[1,5-a]pyrimidines for the study of the peripheral benzodiazepine receptor using positron emission tomography. *J. Med. Chem.* **2008**, *51*, 3700–3712.

(30) Chauveau, F.; Boutin, H.; Thominiaux, C.; Dollé, F.; Trebossen, R.; Kassiou, M.; Katsifis, A.; Tavitian, B. MicroPET evaluation of new tracers for neuroinflammation imaging. *Mol. Imaging* **2006**, *5*, 433–434.

(31) James, M.; Fulton, R.; Henderson, D.; Eberl, S.; Fulham, M.; Allan, R.; Thompson, S.; Dollé, F.; Kassiou, M. Synthesis and in vivo evaluation of a novel PET radioligand for imaging the peripheral benzodiazepine receptor. *J. Labelled Compd. Radiopharm.* **2005**, *48*, S3.

(32) James, M. L; Fulton, R. R.; Henderson, D. J.; Eberl, S.; Meikle, S. R.; Thomson, S.; Allan, R. D.; Dollé, F.; Fulham, M. J.; Kassiou, M. Synthesis and *in vivo* evaluation of a novel peripheral benzodiazepine receptor PET radioligand. *Bioorg. Med. Chem*. **2005**, *13*, 6188–6194.

(33) Thominiaux, C.; Dollé, F.; James, M. L.; Bramoullé, Y.; Boutin, H.; Besret, L.; Grégoire, M. C.; Valette, H.; Bottlaender, M.; Tavitian, B.; Hantraye, P.; Selleri, S.; Kassiou, M. Improved synthesis of the peripheral benzodiazepine receptor ligand [^{11}C]DPA-713 using [^{11}C]methyl triflate. *Appl. Radiat. Isot.* **2006**, *64*, 570–573.

(34) Boutin, H.; Chauveau, F.; Thominiaux, C.; Grégoire, M.-C.; James Michelle, L.; Trebossen, R.; Hantraye, P.; Dollé, F.; Tavitian, B.; Kassiou, M. ^{11}C-DPA-713: A novel peripheral benzodiazepine receptor PET ligand for *in vivo* imaging of neuroinflammation. *J. Nucl. Med.* **2007**, *48*, 573−581.

(35) Bennacef, I.; Salinas, C. A.; Jensen, S. B.; Cunningham, V. J.; Bonasera, T. A.; Gee, A. D. [^{11}C]DPA713: Radiosynthesis and evaluation for cerebral peripheral benzodiazepine receptor imaging. *J. Labelled Compd. Radiopharm.* **2007**, *50*, S341.

(36) James, M. L.; Fulton, R.; Vercouillie, J.; Henderson, D.; Garreau, L.; Eberl, S.; Chalon, S.; Selleri, S.; Dollé, F.; Guilloteau, D.; Kassiou, M. DPA-714, a new translocator protein (18 kDa) ligand: Synthesis, radiofluorination and pharmacological characterisation. *J. Labelled Compd. Radiopharm.* **2007**, *50*, S25.

(37) Doorduin, J.; Klein, H. C.; James, M. L.; Kassiou, M.; Dierckx, R. A.; De Vries, E. F. J. [^{18}F]DPA-714 as a novel PET tracer for PBR: A comparison with [^{11}C]PK11195 in a rat model of HSV encephalitis. *J. Labelled Compd. Radiopharm.* **2007**, *50*, S333.

(38) James, M. L.; Fulton, R. R.; Vercoullie, J.; Henderson, D. J.; Garreau, L.; Chalon, S.; Dollé, F.; Selleri, S.; Guilloteau, D.; Kassiou, M. DPA-714, a new translocator protein-specific ligand: Synthesis, radiofluorination, and pharmacologic characterization. *J. Nucl. Med.* **2008**, *49*, 814–822.

(39) Damont, A.; Hinnen, F.; Kuhnast, B.; Schollhorn-Peyronneau, M.-A.; James, M. L.; Luus, C.; Tavitian, B.; Kassiou, M.; Dollé, F. Radiosynthesis of [^{18}F]DPA-714, a selective radioligand for imaging the translocator protein (18 kDa) with PET. *J. Labelled Compd. Radiopharm.* **2008**, *51*, 286−292.

(40) Tang, D.; McKinley, E. T.; Hight, M. R.; Uddin, Md. I.; Harp, J. M.; Fu, A.; Nickels, M. L.; Buck, J. R.; Manning, H. C. Synthesis and structure−activity relationships of 5,6,7-substituted

pyrazolopyrimidines: discovery of a novel TSPO PET ligand for cancer imaging. *J. Med. Chem*. **2013**, *56*, 3429–3433.

(41) Tang, D.; Nickels, M. L.; Tantawy, M. N.; Buck, J. R.; Manning, H. C. Preclinical imaging evaluation of novel TSPO-PET ligand 2-(5,7-diethyl-2-(4-(2-[^{18}F]fluoroethoxy)phenyl)pyrazolo[1,5-*a*]pyrimidin-3-yl)-***N***,***N***-diethylacetamide ([^{18}F]VUIIS1008) in glioma. *Mol. Imaging Biol*. **2014**, *16*, 813–820.

(42) Pham, T.; Fookes, C.; Liu, X.; Greguric, I.; Bourdier, T.; Katsifis, A. Synthesis of [^{18}F]Fluorine labelled imidazo[1,2b]pyridazine as potential probes for the study of peripheral benzodiazepine binding sites using PET. *J. Labelled Compd. Radiopharm.* **2007**, *50*, S204.

(43) Romeo, E.; Auta, J.; Kozikowski, A. P.; Ma, D.; Papadopoulos, V.; Puia, G.; Costa, E.; Guidotti, A. 2-Aryl-3-Indoleacetamides (FGIN-1): A new class of potent and specific ligands for the mitochondrial DBI receptor (MDR). *J. Pharmacol. Exp. Ther*. **1992**, *262*, 971–978.

(44) Pike, V. W.; Taliani, S.; Lohith, T. G.; Owen, D. R. J.; Pugliesi, I.; Da Pozzo, E.; Hong, J.; Zoghbi, S. S.; Gunn, R. N.; Parker, C. A.; Rabiner, E. A.; Fujita, M.; Innis, R. B.; Martini, C.; Da Settimo, F. Evaluation of novel N^1-Methyl-2-phenylindol-3-ylglyoxylamides as a new chemotype of 18 kDa translocator protein-selective ligand suitable for the development of positron emission tomography radioligands. *J. Med. Chem*. **2011**, *54*, 366–373.

(45) Thominiaux, C.; Damont, A.; Kuhnast, B.; Demphel, S.; Le Helleix, S.; Boisnard, S. ; Rivron, L.; Chauveau, F. ; Boutin, H.; Van Camp, N.; Boisgard, R.; Roy, S.; Allen, J.; Rooney, T.; Benavides, J.; Hantraye, P.; Tavitian, B.; Dollé, F. Radiosynthesis of 7-chloro-*N*,*N*-dimethyl-5-[^{11}C]methyl-4-oxo-3-phenyl-3,5-dihydro-4*H*-pyridazino[4,5-*b*]indole-1-acetamide, [^{11}C]SSR180575, a novel radioligand for imaging the TSPO (peripheral benzodiazepine receptor) with PET. *J. Labelled Compd. Radiopharm.* **2010**, *53*, 767–773.

(46) Wadsworth, H.; Jones, P. A.; Chau, W. F.; Durrant, C.; Fouladi, N.; Passmore, J.; O'Shea, D.; Wynn, D.; Morisson-Iveson, V.; Ewan, A.; Thaning, M.; Mantzilas, D.; Gausemel, I.; Khan, I.; Black, A.; Avory, M.; Trigg, W. [^{18}F]GE-180: a novel fluorine-18 labelled PET tracer for imaging Translocator protein 18 kDa (TSPO). *Bioorg. Med. Chem. Lett*. **2012**, *22*, 1308−1313.

(47) Zhang, M. R.; Kumata, K.; Maeda, J.; Yanamoto, K.; Hatori, A.; Okada, M.; Higuchi, M.; Obayashi, S.; Suhara, T.; Suzuki, K. 11C-AC-5216: a novel PET ligand for peripheral benzodiazepine receptors in the primate brain. *J. Nucl. Med*. **2007**, *48*, 1853−1861.

(48) Yanamoto, K.; Kumata, K.; Yamasaki, T.; Odawara, C.; Kawamura, K.; Yui, J.; Hatori, A.; Suzuki, K.; Zhang, M.-R. [^{18}F]FEAC and [^{18}F]FEDAC: Two novel positron emission tomography ligands for peripheral-type benzodiazepine receptor in the brain. *Bioorg. Med. Chem. Lett*. **2009**, *19*, 1707−1710.

(49) Peyronneau, M.-A.; Saba, W.; Goutal, S.; Damont, A.; Dollé, F.; Kassiou, M.; Bottlaender, M.; Valette, H. Metabolism and quantification of [^{18}F]DPA-714, a new TSPO positron emission tomography radioligand. *Drug Metab. Dispos.* **2013**, *41*, 122−131.

(50) Eun, L.; Chulbom, L.; Jin, S. T.; Ho, S. W.; S. L. Kap. Radical isomerization via intramolecular ipso substitution of aryl ethers: Aryl translocation from oxygen to carbon. *Tetrahedron Lett*. **1993**, *34*, 2343−2346.

(51) Leeson, P. D.; Springthorpe, B. The influence of drug-like concepts on decision making in medicinal chemistry. *Nat. Rev. Drug Discovery* **2007**, *6*, 881−890.

(52) Chauveau, F.; Van Camp, N.; Dollé, F.; Kuhnast, B.; Hinnen, F.; Damont, A.; Boutin, H.; James, M. L.; Kassiou, M.; Tavitian, B. Comparative evaluation of the translocator protein radioligands ^{11}C-DPA-713, ^{18}F-DPA-714, and ^{11}C-PK11195 in a rat model of acute neuroinflammation. *J. Nucl. Med*. **2009**, *50*, 468−476.

(53) Kuhnast, B.; Damont, A.; Hinnen, F.; Catarina, T.; Demphel, S.; Le Helleix, S.; Coulon, C.; Goutal, S.; Gervais, P.; Dollé, F. [^{18}F]DPA-714, [^{18}F]PBR111 and [^{18}F]FEDAA1106 - Selective radioligands for imaging TSPO 18 kDa with PET: Automated radiosynthesis on a TRACERLab FX-FN synthesizer and quality controls. *Appl. Radiat. Isot.* **2012**, *70*, 489–497.

(54) Cointepas, Y.; Mangin, J.-F.; Garnero, L.; Poline, J.-B.; Benali, H. BrainVISA: Software platform for visualization and analysis of multi-modality brain data. *Neuroimage* **2001**, *13*, S98.

Table of contents graphic